Multiqubit monogamy relations beyond shadow inequalities

Eduardo Serrano-Ensástiga, ^{1,*} Olivier Giraud, ^{2,3,4,†} and John Martin^{1,‡}

¹Institut de Physique Nucléaire, Atomique et de Spectroscopie, CESAM, University of Liège

B-4000 Liège, Belgium

²Université Paris-Saclay, CNRS, LPTMS, 91405, Orsay, France

³MajuLab, CNRS-UCA-SU-NUS-NTU International Joint Research Laboratory

⁴Centre for Quantum Technologies, National University of Singapore, 17543 Singapore, Singapore

(Dated: July 17, 2025)

Multipartite quantum systems are subject to monogamy relations that impose fundamental constraints on the distribution of quantum correlations between subsystems. These constraints can be studied quantitatively through sector lengths, defined as the average value of m-body correlations, which have applications in quantum information theory and coding theory. In this work, we derive a set of monogamy inequalities that complement the shadow inequalities, enabling a complete characterization of the numerical range of sector lengths for systems with $N \leq 5$ qubits in a pure state. This range forms a convex polytope, facilitating the efficient extremization of key physical quantities, such as the linear entropy of entanglement and the quantum shadow enumerators, by a simple evaluation at the polytope vertices. For larger systems $(N \geq 6)$, we highlight a significant increase in complexity that neither our inequalities nor the shadow inequalities can fully capture.

I. INTRODUCTION

The constituents of a multipartite quantum system exhibit correlations, some of which arise solely from their quantum nature. These correlations include entanglement, which has no classical analogue. However, quantum correlations are not arbitrary but are subject to fundamental physical constraints. A well-known example is the monogamy of entanglement in three-qubit systems [1, 2], which restricts how entanglement is shared among three qubits, thereby limiting the ability of each qubit to be entangled with more than one other. More generally, multipartite quantum systems obey similar monogamy relations that limit the distribution of quantum correlations between subsystems. These correlations are essential resources for applications in quantum metrology and quantum information processing. It is therefore very interesting to characterize and quantify them, assuming only that the global state is pure.

For multiqubit systems, a general state ρ is fully specified by the expectation values of Pauli strings,

$$\sigma_{\boldsymbol{\mu}} = \sigma_{\mu_1 \mu_2 \dots \mu_N} = \sigma_{\mu_1} \otimes \dots \otimes \sigma_{\mu_N} \,, \tag{1}$$

where σ_0 denotes the identity operator and σ_a (a=1,2,3) are the Pauli matrices, and each index μ_{α} takes values in $\{0,1,2,3\}$. Constraints on quantum correlations are therefore encoded in the expectation values $\langle \sigma_{\mu} \rangle$. Grouping these expectation values according to the number of non-identity Pauli operators forms the basis for defining the sector lengths S_m [3–5]. These quantify the average correlations between m qubits in the N-qubit system. More precisely, they are defined as the average of

the squared expectation values of the Pauli strings that act in a non-trivial way on the qubits. Although these quantities are far fewer in number than Pauli strings, they have many practical applications, including the detection of m-partite entanglement [4–13], generalized uncertainty relations [14–16], quantum secret sharing [17], the quantum marginal problem [18], and noise robustness of entanglement [19], among others [20].

Sector lengths were originally introduced within the framework of quantum coding theory [21], where they are more commonly referred to as Shor-Laflamme enumerators [22]. In this context, S_m quantifies the effect of errors acting simultaneously on m qubits [21, 23– 28]. As such, the numerical values that S_m can take determine the feasibility of constructing quantum codes, and, conversely, constraints on quantum codes impose bounds on the sector lengths. Several key bounds on quantum codes, and thus on sector lengths, include the quantum analogs of classical results such as the Hamming bound [23], the singleton bound [24], and the MacWilliams identities [21, 27]. Additional constraints arise from quantum shadow enumerators [26, 27], whose physical interpretation and experimental measurement have been recently explored in [29]. In particular, certain classes of highly entangled states, such as absolutely maximally entangled (AME) states [17, 30–36] and muniform states [22, 33, 37–43], are associated with optimal quantum error-correcting codes [22, 36, 44–46].

In this work, we derive multiqubit monogamy relations in the form of inequalities involving only sector lengths. By combining these inequalities with those already known, we obtain a set of constraints that, in certain cases, fully characterize the realizable values of sector lengths for pure states. For systems with up to five qubits, we show that the set of achievable sector lengths forms a polytope. Similar polytope structures have already been found for mixed states of two and three qubits in Ref. [5]. This complete characterization allows us to

^{*} ed.ensastiga@uliege.be

 $^{^{\}dagger}$ olivier.giraud@universite-paris-saclay.fr

[‡] jmartin@uliege.be

efficiently optimize various quantities related to entanglement and quantum correlations over all pure states with these numbers of qubits. Furthermore, we highlight several connections between sector lengths, linear entanglement entropy, and quantum shadow enumerators.

The paper is organized as follows. In Sec. II, we review basic monogamy relations involving sector lengths. In Sec. III, we derive additional monogamy relations based on the time-reversed state. In Secs IV and VI, we examine the numerical values that sector lengths can take for systems with up to N=6 qubits and explore their relevance to entanglement theory, quantum coding theory, and the verification of monogamy conjectures. Finally, Section VII presents our conclusions and perspectives.

II. DEFINITIONS AND BASIC INEQUALITIES

A. Sector lengths and general inequalities

Consider an arbitrary N-qubit state ρ . We expand ρ in the Pauli string basis (1) as

$$\rho = \frac{1}{2^N} \sum_{\mu} x_{\mu} \sigma_{\mu} \,, \tag{2}$$

where the coefficients $x_{\mu} = \text{Tr} (\rho \sigma_{\mu})$ are real numbers. Throughout this work, we follow the convention that Greek indices run from 0 to 3, while Latin indices are restricted to the range 1 to 3. The weight of a Pauli string, denoted by $\text{wt}(\sigma_{\mu})$, is defined as the number of non-zero indices in the multi-index μ [25]. Accordingly, a correlation involving m parties corresponds to a Pauli string with $\text{wt}(\sigma_{\mu}) = m$.

Consider a subset $A \subset \{1, \ldots, N\}$ of k qubits. We denote by ρ_A the reduced density matrix obtained by tracing out the complementary set $\bar{A} = \{1, \ldots, N\} \setminus A$, *i.e.*, the qubits not in A. A useful property of the parametrization (2) is that the coefficients $x_{\mu_1...\mu_k}^A$ of ρ_A are directly inherited from those of ρ , with zeros inserted in place of the indices associated with \bar{A} . For example, when tracing out the last N - k qubits, we have $A = \{1, \ldots, k\}$ and

$$x_{\mu_1...\mu_k}^A = x_{\mu_1...\mu_k 0...0} = x_{\mu_1...\mu_k 0_{N-k}}$$
 (3)

where $\mathbf{0}_{N-k}$ denotes a string of N-k zeros [37, 47].

The sector length S_m is defined as the sum of the squared coefficients corresponding to m-body correlations,

$$S_m \equiv \sum_{\text{wt}(\sigma_{\mu})=m} x_{\mu}^2. \tag{4}$$

They define positive numbers,

$$S_m \geqslant 0, \quad \text{for } m = 1, \dots, N$$
 (5)

since they are a sum of squares. However, the values of S_m are not arbitrary when ρ varies over the set of valid

density matrices. Their allowed ranges are constrained by the fundamental properties of ρ , including positivity, normalization, and (if applicable) purity. For example, normalization of ρ implies that

$$S_0 = \text{Tr}(\rho)^2 = 1.$$
 (6)

The purity of ρ can be expressed in terms of the S_m as

$$\operatorname{Tr}(\rho^{2}) = \frac{1}{2^{N}} \sum_{m=0}^{N} \sum_{\operatorname{wt}(\sigma_{\mu})=m} x_{\mu}^{2}$$

$$= \frac{1}{2^{N}} (S_{0} + S_{1} + S_{2} + \dots + S_{N}),$$
(7)

where we have used the orthonormality of the Pauli string basis and the expansion of ρ in Eq. (2). Since $\text{Tr}(\rho^2)$ is bounded between 2^{-N} and 1 for any density matrix, this yields the constraint

$$1 \le S_0 + S_1 + S_2 + \ldots + S_N \le 2^N, \tag{8}$$

where the upper bound is achieved for pure states, while the lower bound is achieved for the maximally mixed state. Additional constraints on the sector lengths can be derived based the time-reversed density matrix [11]

$$\tilde{\rho} \equiv \sigma_u^{\otimes N} \rho^* \sigma_u^{\otimes N} \,, \tag{9}$$

where * denotes complex conjugation. The quantity

$$R_{\rho} \equiv \text{Tr}(\rho \tilde{\rho}) = \frac{1}{2^N} \sum_{\mu} x_{\mu} x^{\mu}$$
 (10)

defines the overlap between the density matrix ρ and its time-reversed counterpart $\tilde{\rho}$. Here, we introduced the dual coefficients $x^{\mu} = \sum_{\nu} g^{\mu\nu} x_{\nu}$, where the metric tensor is defined as a product of single-qubit $g^{\mu\nu} = \text{diag}(1,-1,-1,-1)$. Expressed in terms of the sector lengths S_m , R_{ρ} takes the form [11]

$$R_{\rho} = \frac{1}{2^{N}} \left[S_0 - S_1 + S_2 - \dots + (-1)^N S_N \right] . \tag{11}$$

Since $R_{\rho} \ge 0$ for all physical states, combining this with the purity constraint in Eq. (8) yields the inequality

$$0 \leqslant S_0 - S_1 + S_2 - \ldots + (-1)^N S_N \leqslant 2^N.$$
 (12)

B. Constraints for pure states

For a pure state $\rho = |\psi\rangle\langle\psi|$, the values of S_m are further constrained by the fact that $\text{Tr}(\rho^2) = 1$, which produces

$$\sum_{m=0}^{N} S_m = 2^N \,. \tag{13}$$

Moreover, for any odd number of qubits N, the timereversed state

$$|\tilde{\psi}\rangle = \sigma_y^{\otimes N} |\psi^*\rangle \tag{14}$$

is orthogonal to the original pure state $|\psi\rangle$ [11, 48]. Therefore, the overlap $R_{\rho} = |\langle\psi|\tilde{\psi}\rangle|^2 = 0$, and Eq. (12) yields

$$\sum_{m=0}^{N} (-1)^m S_m = 0, \quad \text{for } N \text{ odd.}$$
 (15)

We now turn to the reduced states obtained by taking partial traces of ρ . For any bipartition $A \cup \bar{A} = \{1, \ldots, N\}$, the purities of the reduced density matrices ρ_A and $\rho_{\bar{A}}$ are equal, $\text{Tr}(\rho_A^2) = \text{Tr}(\rho_{\bar{A}}^2)$. This equality leads to the following set of identities [18, 21]

$$\frac{1}{2^{N-k}} \sum_{m=0}^{N-k} {N-m \choose k} S_m = \frac{1}{2^k} \sum_{m=0}^k {N-m \choose N-k} S_m, \quad (16)$$

valid for all $k=0,\ldots,N$. A full derivation of Eq. (16) is provided in Appendix A. These relations represent an alternative formulation of the MacWilliams identity, a well-known result in classical coding theory [21, 25, 35]. Importantly, they allow one to express the sector lengths S_m for $m>\lfloor N/2\rfloor$ in terms of those with $m\leqslant \lfloor N/2\rfloor$, significantly reducing the number of independent S_m .

C. Shadow inequalities

Additional constraints on the sector lengths of pure and mixed N-qubit states are given by the so-called quantum shadow inequalities [18, 26, 27], which take the form

$$S_g^{(e)}(\rho) \equiv \frac{1}{2^N} \sum_{m=0}^N (-1)^m K_g(m, N) S_m(\rho) \geqslant 0,$$
 (17)

for all g = 0, ..., N, and where $K_g(m, N)$ are known as Kravchuk polynomials [26, 49, 50], defined by

$$K_g(m,N) \equiv \sum_{i=0}^{g} (-1)^i 3^{g-i} {m \choose i} {N-m \choose g-i}.$$
 (18)

The quantities $S_g^{(e)}$ are called *shadow enumerators*. In particular, for g=0, we recover the overlap with the time-reversed state

$$S_0^{(e)}(\rho) = R_{\rho} \geqslant 0.$$
 (19)

The inverse relation of Eq. (17) is given by (see Appendix B for a detailed derivation)

$$S_m = \frac{(-1)^m}{2^N} \sum_{g=0}^N K_m(g, N) S_g^{(e)}.$$
 (20)

We explain in more detail the connection between the inequalities (17) and quantum coding theory in Appendix B. It should be noted that the inequalities (17) can also be derived independently of the quantum coding framework using a representation of sector lengths in the double-copy Hilbert space. For the sake of completeness, this alternative derivation is included in Appendix C.

D. Numerical range

Taking into account the positivity condition (5) and the normalization condition (6), the sector length vector $\mathbf{S} \equiv (S_1, \dots, S_N)$ lies within a subset of \mathbb{R}^N_+ . We define the numerical range of sector lengths for pure states as

$$S \equiv \left\{ \mathbf{S}(\rho) \middle| \rho = |\psi\rangle \langle \psi| \right\} \subset \mathbb{R}_{+}^{N} . \tag{21}$$

The main aim of our work is to characterize S as completely as possible by deriving inequalities that capture the monogamy of quantum correlations in pure multiqubit states. To that end, we define \mathcal{R}_1 as the subset of vectors in \mathbb{R}_+^N that satisfy the conditions specific to pure states given in Sections II A and II B:

$$\mathcal{R}_1 = \left\{ \mathbf{S} \in \mathbb{R}_+^N \middle| \text{Eqs. (13), (15), (16) hold} \right\}.$$
 (22)

The shadow inequalities (17) for g = 0, ..., N impose additional constraints on \mathbf{S} , further refining the admissible region to

$$\mathcal{R}_2 = \mathcal{R}_1 \cap \left\{ \mathbf{S} \middle| \text{Eq. (17) holds} \right\}. \tag{23}$$

By definition, we have that $S \subseteq \mathcal{R}_2 \subseteq \mathcal{R}_1$. In the next section, we derive new inequalities that further restrict the allowed values of the sector lengths S_m , thereby refining the characterization of S.

III. MONOGAMY INEQUALITIES FROM REDUCED DENSITY MATRICES

In this section, we derive inequalities that complement those in the previous section, starting from the Schmidt decomposition of a pure state. This will give inequalities associated with the reduced density matrices of $|\psi\rangle$ whose purities are related to the sector lengths.

A. Inequalities for reduced density matrices

Consider a pure state $|\psi\rangle$ of N qubits, and a bipartition $A|\bar{A}$ that splits the system into k and N-k qubits. The Schmidt decomposition of $|\psi\rangle$ with respect to this bipartition reads

$$|\psi\rangle = \sum_{i=1}^{2^{\min(k,N-k)}} \sqrt{p_i} |\phi_i\rangle \otimes |\chi_i\rangle,$$
 (24)

with $p_i \geqslant 0$, $\sum_i p_i = 1$, and $\{|\phi_i\rangle\}_i$ and $\{|\chi_i\rangle\}_i$ forming orthonormal sets of states in the subsystems A and \bar{A} , respectively. By tracing over subsystem \bar{A} , we obtain the reduced density matrix $\rho_A = \sum_i p_i |\phi_i\rangle \langle \phi_i|$, and therefore

$$\operatorname{Tr}(\rho_A^2) = \sum_i p_i^2 = 1 - 2 \sum_{i < j} p_i p_j,$$
 (25a)

$$R_{\rho_A} = \text{Tr}(\rho_A \tilde{\rho}_A) = \sum_{i,j} p_i p_j |\langle \phi_i | \tilde{\phi}_j \rangle|^2.$$
 (25b)

where $|\tilde{\phi}_j\rangle$ is defined as in Eq. (14). Using the fact that the purities of ρ_A and $\rho_{\bar{A}}$ are equal for any pure bipartite state $|\psi\rangle$ and minimal when the reduced state of the smallest subsystem is maximally mixed, Eq. (25) implies the following inequalities

$$\frac{1}{2^{\min(k,N-k)}} \leqslant \text{Tr}(\rho_A^2) \leqslant 1, \tag{26a}$$

$$0 \leqslant R_{\rho_A} \leqslant 1. \tag{26b}$$

As noted in section IIB, for any odd k, a k-qubit state $|\phi\rangle$ is orthogonal to its time-reversed state $|\tilde{\phi}\rangle$. Thus, for odd k, the expression for R_{ρ_A} simplifies to $2\sum_{i< j} p_i p_j |\langle \phi_i | \tilde{\phi}_j \rangle|^2$. Combining with Eq. (25a), we obtain

$$1 - \text{Tr}(\rho_A^2) - R_{\rho_A} = 2 \sum_{i < j} p_i p_j \left(1 - |\langle \phi_i | \tilde{\phi}_j \rangle|^2 \right) \geqslant 0.$$
 (27)

Summing Eqs. (26a) and (26b), we get

$$2^{-\min(k,N-k)} \leqslant \text{Tr}(\rho_A^2) + R_{\rho_A} \leqslant \frac{3 + (-1)^k}{2}$$
 (28)

where, for odd k, the upper bound follows from Eq. (27).

B. Sector length inequalities

The quantities $\text{Tr}(\rho_A^2)$ and R_{ρ_A} in (28) can be expressed in terms of the sector lengths $S_m(\rho_A)$. Indeed, using Eqs. (7) and (11) for ρ_A (a k-qubit state), we get

$$\operatorname{Tr}(\rho_A^2) = \frac{1}{2^k} \sum_{m=0}^k S_m(\rho_A),$$

$$R_{\rho_A} = \frac{1}{2^k} \sum_{m=0}^k (-1)^m S_m(\rho_A).$$
(29)

In order to obtain additional inequalities for the sector lengths of the pure state $\rho = |\psi\rangle \langle \psi|$ of which ρ_A is a reduction, we consider sums over all sets A with k elements. For fixed k and $m \leq k$, the sector lengths $S_m(\rho_A)$ of the reduced states and the sector lengths $S_m(\rho)$ of the pure state are related by the identity

$$\sum_{|A|=k} S_m(\rho_A) = {N-m \choose k-m} S_m(\rho) \quad \forall m \leqslant k, \qquad (30)$$

where |A| denotes the cardinality of A. A proof of (30) is given in Appendix A. By summing (29) over all subsets of length k and using (30), we obtain

$$\sum_{|A|=k} \text{Tr}(\rho_A^2) = \frac{1}{2^k} \sum_{m=0}^k {N-m \choose k-m} S_m(\rho),$$
 (31)

$$\sum_{|A|=k} R_{\rho_A} = \frac{1}{2^k} \sum_{m=0}^k (-1)^m \binom{N-m}{k-m} S_m(\rho).$$
 (32)

Summing Eqs. (26a), (26b) and (28) in the same way, we get

$$\frac{1}{2^{\min(k,N-k)}} \binom{N}{k} \leqslant \sum_{|A|=k} \operatorname{Tr}(\rho_A^2) \leqslant \binom{N}{k},$$

$$0 \leqslant \sum_{|A|=k} R_{\rho_A} \leqslant \binom{N}{k},$$

$$\frac{\binom{N}{k}}{2^{\min(k,N-k)}} \leqslant \sum_{|A|=k} \left[\operatorname{Tr}(\rho_A^2) + R_{\rho_A}\right] \leqslant \frac{3 + (-1)^k}{2} \binom{N}{k}.$$
(33)

This leads to new constraints on the sector lengths that must be satisfied by any pure multiqubit state:

$$\frac{2^k}{2^{\min(k,N-k)}} \binom{N}{k} \leqslant \sum_{m=0}^k \binom{N-m}{k-m} S_m \leqslant 2^k \binom{N}{k}, \quad (34)$$

$$0 \leqslant \sum_{m=0}^{k} (-1)^m {N-m \choose k-m} S_m \leqslant 2^k {N \choose k}, \tag{35}$$

$$\sum_{m=0}^{\lfloor \frac{k-1}{2} \rfloor} {N-2m \choose k-2m} S_{2m} \leqslant 2^{k-2} \left(3 + (-1)^k\right) {N \choose k}.$$
 (36)

Equations (34)–(36) define a new region in the **S** space that further restricts the admissible values of the sector lengths. We denote this region by

$$\mathcal{R}_3 = \mathcal{R}_1 \cap \left\{ \mathbf{S} \mid \text{Eqs. (34)-(36) hold } \forall \ k = 1, \dots, N \right\}.$$

We note that the upper bound in Eq. (34) and the lower bound in Eq. (35) were previously established in Proposition 7 and Eq. (32) of Ref. [18].

C. Summary of our results

We summarize our main result in the following theorem.

Theorem 1 Let

$$\mathcal{R} = \mathcal{R}_2 \cap \mathcal{R}_3 \,, \tag{38}$$

where \mathcal{R}_2 and \mathcal{R}_3 are the subsets of \mathbb{R}^N_+ defined in Eqs. (23) and (37), respectively. Then, \mathcal{R} defines a polytope and the set \mathcal{S} of achievable sector length vectors for pure states is contained within this polytope, that is,

$$S \subset \mathcal{R}.$$
 (39)

Although numerical optimization of S_m on the simplex \mathcal{R} is relatively straightforward, finding the extremal values of S_m within the set \mathcal{S} involves optimizing a quartic polynomial in 2N variables (the real and imaginary parts of the components of $|\psi\rangle$). This is computationally feasible only for a small number of qubits.

We performed a numerical optimization to determine the extremal values of the S_m and the corresponding pure states that achieve these optima, for $m=1,2,\ldots,N$ on systems of $N=1,\ldots,8$ qubits. The results are summarized in Table III. The states highlighted in gray can be shown analytically to saturate the bounds defining the set \mathcal{R} . Since $\mathcal{S} \subset \mathcal{R}$, this confirms that these states are indeed the optimal pure states within \mathcal{S} . Some of these optimal states were previously known, with references provided in Table III.

The following list presents results that, to our knowledge, have not been reported before:

- For N = 4, S is completely characterized and coincides with R. Its shape is a polytope.
- For N=5, the boundaries of \mathcal{S} are fully characterized, and strong numerical evidence suggests that \mathcal{S} coincides with the polytope \mathcal{R} .
- For N=5 and N=6, it is known that absolutely maximally entangled (AME) states satisfy $S_2=0$. Furthermore, we show that the specific AME states given in Eqs. (E4) and (E8) also achieve the global maximum of S_4 . It should be noted that there are other 6-qubit AME states that do not achieve this maximum.
- For N = 5, the global minimum of S_4 is reached by a product state.
- For N=6, the symmetric state given in Eq. (E12) maximizes S_5 .
- For N=7, the state $|\mathrm{AME}(6,2)\rangle|0\rangle$ with $|\mathrm{AME}(6,2)\rangle$ given in Eq. (E8) minimizes S_2 .
- For N=8, the state $|\psi_M\rangle_{12783456}$ given in Eq. (E20) minimizes S_2 .
- We prove Conjecture 2, which concerns the maximum of S_m , for m=4 and m=5.

Furthermore, we derive another proof that the maximum value of S_N is equal to $2^{N-1} + 1$ for N even. This result was conjectured in Ref. [7] and later proved in Ref. [51]. Our alternative proof is presented in Subsection VD and is based entirely on our inequalities.

IV. MONOGAMY RELATIONS FOR SMALL NUMBERS OF QUBITS

In this section, we apply Theorem 1 to determine the numerical range S of the sector lengths of pure multiqubit states (21). Our analysis focuses on systems between 2 and 6 qubits. For $N \leq 5$, we show that S forms a polytope. In these cases, we also identify the extremal quantum states corresponding to the vertices and edges of the respective polytopes. However, the case N = 6 presents

a significantly more complicated scenario, and we are unable to verify that $\mathcal S$ retains a polytope structure. Table I summarizes optimal quantum states associated with the extremal points of the set $\mathcal R$ for all $N \leqslant 6$. These states account for all upper bounds reported in Table III, and also for all lower bounds, with the exception of the bound $S_4 \geqslant 5$ for N=6. To express these results, we make use of the generalized GHZ state, defined as

$$|GHZ(N,\phi)\rangle \equiv \cos\left(\frac{\phi}{2}\right)|0\rangle^{\otimes N} + \sin\left(\frac{\phi}{2}\right)|1\rangle^{\otimes N}$$
 (40)

with $\phi \in [0, \pi]$. We denote the standard N-qubit GHZ state by $|\text{GHZ}(N)\rangle \equiv |\text{GHZ}(N, \frac{\pi}{2})\rangle$.

A. 2 qubits

In this case, $\mathcal{R}_1 \subset \mathbb{R}^2_+$ is defined by the following non-trivial (in)equalities

$$S_1 + S_2 = 3, \qquad 0 \leqslant 1 - S_1 + S_2 \leqslant 4.$$
 (41)

These conditions imply that $S_1 \in [0, 2]$, $S_2 \in [1, 3]$, and that S_1 and S_2 are linearly related. The sets \mathcal{R}_2 and \mathcal{R}_3 coincide with \mathcal{R}_1 , so all three are fully characterized by the constraints (41). For the generalized GHZ state $|\text{GHZ}(2,\phi)\rangle$, the sector lengths are given by $S_1 = 2\cos^2\phi$ and $S_2 = 3 - 2\cos^2\phi$. When ϕ varies, these expressions span the set of allowed values (S_1, S_2) , with the extremal values being achieved by product states and by the $|\text{GHZ}(2)\rangle$ state. This shows that each point in \mathcal{R} corresponds to a pure state. It follows that $\mathcal{S} = \mathcal{R}$, and that the entire set \mathcal{S} can be parametrized by the angle ϕ .

B. 3 qubits

For three qubits, the set $\mathcal{R}_1 \subset \mathbb{R}^3_+$ is defined by the constraints

$$S_2 = 3, S_1 + S_3 = 4. (42)$$

The smaller sets \mathcal{R}_2 and \mathcal{R}_3 coincide, and differ from \mathcal{R}_1 by the additional inequality

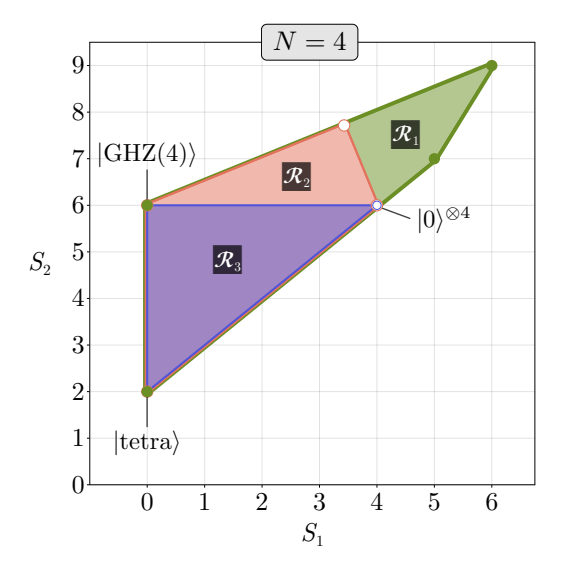
$$0 \leqslant S_1 \leqslant 3. \tag{43}$$

Thus, it follows that $\mathcal{R} = \mathcal{R}_2 = \mathcal{R}_3$ is delimited by the intervals $S_1 \in [0,3]$ and $S_3 \in [1,4]$, with $S_2 = 3$. As in the case of 2 qubits, the family of states $|GHZ(3,\phi)\rangle$ leads to $S_1 = 3\cos^2\phi$, which spans the entire interval \mathcal{R} . Therefore, $\mathcal{R} = \mathcal{S}$, with the extremal values attained by product states and the $|GHZ(3)\rangle$ state.

C. 4 qubits

For four qubits, $\mathcal{R}_1 \subset \mathbb{R}^4_+$ is specified by the equalities

$$S_4 = 3 - 2S_1 + S_2, \qquad S_3 = 12 + S_1 - 2S_2,$$
 (44)



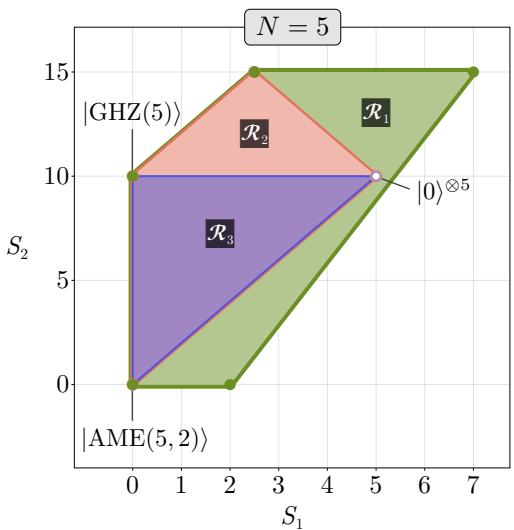


FIG. 1. Projection of the sets $\mathcal{R}_3 \subset \mathcal{R}_2 \subset \mathcal{R}_1$ onto the (S_1, S_2) plane for N=4 (top) and N=5 qubits (bottom), colored in purple, red and green, respectively. For these particular numbers of qubits, $\mathcal{R}=\mathcal{R}_3$ and every point in \mathcal{R}_3 corresponds to a physically realizable quantum state.

and the inequality

$$2 \leqslant S_2 - S_1 \leqslant 6. \tag{45}$$

In Fig. 1, we plot the projection of \mathcal{R}_1 in the sector length subspace (S_1, S_2) (shown as the largest green region). While the set \mathcal{R}_2 (shown in red) is reduced by the additional inequality $3S_1 + S_2 \leq 18$, the set \mathcal{R}_3 (shown in purple) is reduced by an even stricter inequality $S_2 \leq 6$, such that $\mathcal{R} = \mathcal{R}_3 \subset \mathcal{R}_2 \subset \mathcal{R}_1$. The intervals delimiting the set \mathcal{R}_3 are $S_1 \in [0,4]$, $S_2 \in [2,6]$, $S_3 \in [0,8]$, and $S_4 \in [1,9]$, with the limits reached by the states indicated in Table III. It should be noted that this case has also been studied in Refs. [52, 53].

The set $\mathcal{R} = \mathcal{R}_3$, which is entirely characterized by the

conditions

$$0 \leqslant S_1 \leqslant S_2 - 2 \leqslant 4,\tag{46}$$

corresponds to the purple triangle in the top panel of Fig. 1. A family of states that explicitly realizes all points in \mathcal{R} is

$$|\psi_4(\theta,\phi)\rangle = \cos\left(\frac{\theta}{2}\right)|\text{GHZ}(4,\phi)\rangle + i\sin\left(\frac{\theta}{2}\right)|D_4^{(2)}\rangle$$
 (47)

with $\theta \in [0, \frac{\pi}{2}[, \phi \in [0, 2\pi], \text{ and the symmetric Dicke state } |D_4^{(2)}\rangle$ as defined in Eq. (E1). For the family (47), the sector lengths are

$$S_1 = (1 + \cos \theta)^2 \cos^2 \phi, \tag{48}$$

$$S_2 = 2 \left[3 - (1 + \sin \phi) \sin^2 \theta \right].$$
 (49)

To show that Eqs. (48)–(49) parametrize the whole set \mathcal{R} , we let $u = \cos \theta$ and $v = \sin \phi$, which yields

$$S_1 = (1+u)^2 (1-v^2) \equiv x,$$

$$3 - S_2/2 = (1+v)(1-u^2) \equiv y.$$
(50)

Equations (46) yield $0 \leqslant y \leqslant 2 - x/2 \leqslant 2$. We thus want to show that for any $x, y \geqslant 0$ such that $x + 2y \leq 4$ one can find $u \in [0,1]$ and $v \in [-1,1]$ such that $x = (1+u)^2(1-v^2)$ and $y = (1+v)(1-u^2)$. If y = 0 we take u = 1 and $v \in [-1, 1]$. Otherwise, we get in particular the condition $v = 1 - \frac{x(1-u)}{y(1+u)}$, and u must be a root of the order-2 polynomial $P(u) = (x+2y)u^2$ $2ux + x - 2y + y^2$. This polynomial reaches its minimum at $u_0 = x/(x+2y) \in [0,1]$. The condition $x+2y \leq 4$ implies that $P(u_0) = y^2(x+2y-4)/(x+2y) \le 0$, which, together with $P(1) = y^2 \ge 0$, ensures that there is a real root $u \in [u_0, 1]$. To show that the corresponding $v = 1 - \frac{x(1-u)}{y(1+u)}$ is in [-1,1] one needs to check that $x(1-u) \leqslant 2y(1+u)$, that is, $u \geqslant u_0 - 2y/(x+2y)$. This is true since $u \ge u_0$ and $x, y \ge 0$. Thus there exists a solution (u, v) inverting Eq. (50). This shows that $\mathcal{S} = \mathcal{R}$ is given by (46) and parametrized by the two angles θ and ϕ according to (48)–(49). In particular, the maximum of S_1 is achieved by the state $|\psi_4(0,0)\rangle = |0\rangle^{\otimes 4}$. The minimum of S_1 can be reached, for instance, by $|\psi_4(0,\pi/2)\rangle = |\text{GHZ}(4)\rangle$. Lastly, min $S_2 = 2$ is achieved by the state $|\psi_4(\pi/2,\pi/2)\rangle = |\text{tetra}\rangle$ (see Eq. (E2) for more details).

D. 5 qubits

In this case, $\mathcal{R}_1 \subset \mathbb{R}^5_+$ is defined by the equalities

$$S_3 = 10 + 2S_1 - S_2,$$

 $S_4 = 15 - S_2,$ (51)
 $S_5 = 6 - 3S_1 + S_2.$

and the inequalities

$$S_2 \leqslant 15, \quad 3S_1 - 6 \leqslant S_2 \leqslant 2S_1 + 10.$$
 (52)

 \mathcal{R}_2 is constrained by the two additional inequalities

$$2S_1 \leqslant S_2, \qquad 2S_1 + S_2 \leqslant 20.$$
 (53)

Finally, \mathcal{R}_3 is characterized by the above inequalities, together with the additional condition $S_1 \leq 10$. In Fig. 1 we plot the projection onto the (S_1, S_2) plane of the sets $\mathcal{R}_3 \subset \mathcal{R}_2 \subset \mathcal{R}_1$. The intervals of the sector lengths S_m are $S_1 \in [0, 5]$, $S_2 \in [0, 10]$, $S_3 \in [0, 10]$, $S_4 \in [5, 15]$ and $S_5 \in [1, 16]$. The endpoints of these intervals are reached by the examples given in Table III.

The region \mathcal{R} is now characterized by the conditions

$$0 \le S_1 \le 5, \qquad 2S_1 \le S_2 \le 10, \tag{54}$$

corresponding to the purple triangle in Fig. 1 (bottom panel). As shown in the previous subsections, for $N \leq 4$ one can realize all points in \mathcal{R} by simply considering a family of pure states made of superpositions of extremal points. This is no longer the case for N=5, and finding a state realizing an arbitrary point of the domain \mathcal{R} is far from trivial.

Let us consider the left boundary of \mathcal{R} , that is, points for which $S_1=0$ and $0\leqslant S_2\leqslant 10$. A superposition of the $|\mathrm{GHZ}(5)\rangle$ and $|\mathrm{AME}(5,2)\rangle$ states does not enable to reach all values of S_2 for $S_1=0$. However, we can exhibit a family of states which realizes all points on this boundary. Setting z=tx-(t+1)y, we found that states of the form

$$|\psi\rangle = (0, -tz, 0, x, y, 0, tz, 0, z, 0, z, 0, 0, y, 0, z, -z, 0, -y, 0, 0, z, 0, z, 0, tz, 0, y, -x, 0, tz, 0),$$
(55)

in the computational basis, depending on three parameters x, y, t, are such that $S_1 = 0$. The normalization condition for $|\psi\rangle$ can be rewritten

$$2(2t^{4} + 3t^{2} + 1)x^{2} - 4t(2t^{3} + 2t^{2} + 3t + 3)xy + 2(2t^{4} + 4t^{3} + 5t^{2} + 6t + 5)y^{2} = 1, (56)$$

while S_2 is a polynomial in (x, y, t) given by

$$\frac{1}{8}S_2 = -4t(t+1)^2 \left(8t^5 + 8t^4 + t + 17\right) xy^3
+ 2\left(24t^8 + 48t^7 + 24t^6 + 15t^4 + 70t^3 + 54t^2 - 2t - 1\right) x^2y^2
+ \left(8t^8 + 32t^7 + 48t^6 + 32t^5 + 5t^4 + 4t^3 + 30t^2 + 36t + 21\right) y^4
+ \left(8t^8 + 13t^4 - 2t^2 + 5\right) x^4
- 4t\left(8t^7 + 8t^6 + 9t^3 + 17t^2 - t - 1\right) x^3y.$$
(57)

Analytical minimization and maximization of (57) under the constraint (56) shows that the bounds $S_2 = 0$ and $S_2 = 10$ are reached for $(x, y, t) = (\frac{1}{4}, -\frac{1}{4}, -1)$ and $(-\frac{1}{\sqrt{2}}, 0, 0)$, respectively. By continuity, the family of states (55) covers the whole left boundary of the domain \mathcal{R} . Now consider the oblique boundary of \mathcal{R} on the right, characterized by $S_2 = 2S_1$ with $S_1 \in [0, 5]$. We

present two families of states that, taken together, cover this boundary. First, consider the family of states

$$|\psi(\eta)\rangle = \frac{\cos\eta}{2} (|00011\rangle + |00110\rangle - |10001\rangle + |10100\rangle) + \frac{\sin\eta}{2} (|01000\rangle - |01101\rangle + |11010\rangle + |11111\rangle). (58)$$

These states have sector lengths

$$S_2 = 2S_1 = 2\cos^2(2\eta) \tag{59}$$

and thus cover the segment of the right boundary of \mathcal{R} with $S_1 \in [0,1]$ for $\eta \in [0,\pi/4]$. Second, consider the family of states

$$|\phi(\eta)\rangle = \mathcal{N}\left[\cos(\eta/2)|\psi_5\rangle + \frac{\sin(\eta/2)}{\sqrt{2}}|00000\rangle\right], \quad (60)$$

where $|\psi_5\rangle$ is given in Eq. (E6) and $\mathcal{N} = 2(\sin \eta + \cos \eta + 3)^{-1/2}$ is a normalization constant. These states exhibit sector lengths given by

$$S_2 = 2S_1 = \frac{28\sin\eta - 6\sin(2\eta) - 4\cos\eta - \cos(2\eta) + 37}{(\sin\eta + \cos\eta + 3)^2}.$$
(61)

In this case, S_1 increases monotonically from 1 at $\eta = 0$ to 5 at $\eta = \pi$, covering the right boundary of \mathcal{R} with $S_1 \in [1,5]$. Together, these results show that there are states that realize all the points on the right-hand boundary. Finally, the top boundary of \mathcal{R} is covered by the generalized GHZ state (40) as ϕ varies within $[0, \pi/2]$, yielding sector lengths $S_1 = 5\cos^2 \phi$ and $S_2 = 10$. By forming superpositions of states located at the entire boundary, we find numerically that we can obtain any combination of sector lengths within \mathcal{R} .

This leads us to the following conjecture:

Conjecture 1 For a 5-qubit system, the set of sector lengths attainable by pure states S is exactly the polytope R.

E. 6 qubits

For N = 6, we have 3 free variables S_1 , S_2 , and S_3 , and

$$S_4 = 45 + 10S_1 - 2S_2 - 3S_3,$$

$$S_5 = 3S_3 - 9S_1,$$

$$S_6 = 18 - 2S_1 + S_2 - S_3.$$
(62)

 \mathcal{R}_1 is the subset of \mathbb{R}^6_+ defined by the equalities (62) and the inequalities

$$-8 \le 2S_1 - S_3 \le 0. \tag{63}$$

 \mathcal{R}_2 is constrained by \mathcal{R}_1 together with the following additional inequalities

$$30S_1 \le 8S_2 + 3S_3$$
, $10S_1 + 16S_2 + 3S_3 \le 360$. (64)

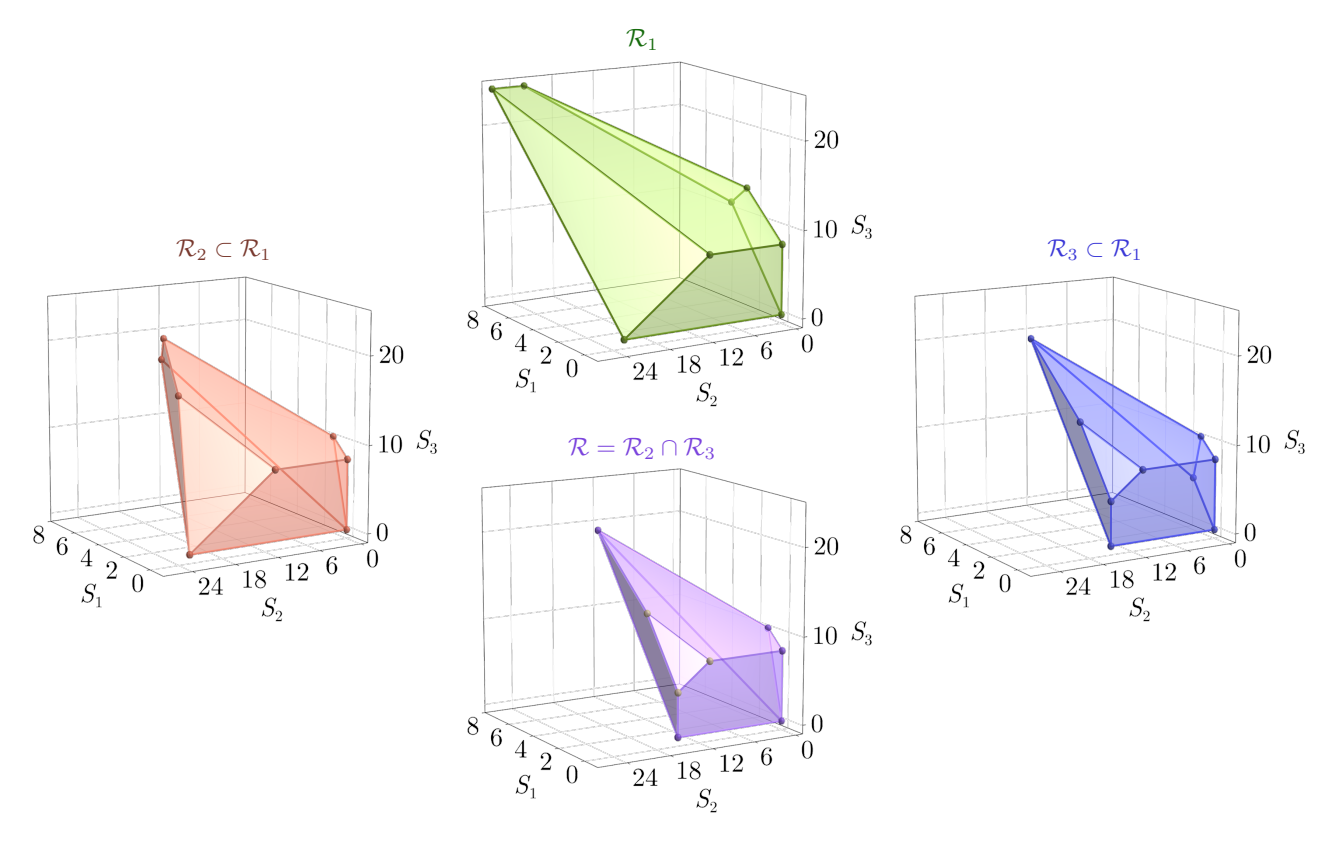


FIG. 2. Projection of the sets \mathcal{R}_1 , $\mathcal{R}_2 \subset \mathcal{R}_1$, $\mathcal{R}_3 \subset \mathcal{R}_1$, and $\mathcal{R} = \mathcal{R}_2 \cap \mathcal{R}_3$ onto the (S_1, S_2, S_3) subspace for N = 6. Note that \mathcal{R}_3 is not contained in \mathcal{R}_2 and vice versa (see the differences in the faces of the polyhedra in the planes $S_2 = 0$ and $S_1 = 0$).

Similarly, \mathcal{R}_3 is constrained by \mathcal{R}_1 together with

$$10S_1 + S_3 - 20 \le 4S_2 \le 60, 10S_1 \le 3S_3. (65)$$

Interestingly, in this case, \mathcal{R}_2 is not contained in \mathcal{R}_3 , as we can observe in Fig. 2. Thus, N=6 is the smallest number of qubits for which $\mathcal{R}=\mathcal{R}_2\cap\mathcal{R}_3\neq\mathcal{R}_3$ and \mathcal{R}_2 . \mathcal{R} has the following ranges in the sector lengths: $S_1\in[0,6],\ S_2\in[0,15],\ S_3\in[0,20],\ S_4\in[0,45],\ S_5\in[0,24]$ and $S_6\in[1,33]$. Our numerical results show that \mathcal{S} is strictly contained in \mathcal{R} , further restricted by $S_4\geqslant 5$ (see Table III). By integrating this constraint into the region \mathcal{R} , along with additional linear constraints derived from numerical optimization, we obtain a reduced polytope in \mathbb{R}^6_+ (see the lower panel of Fig. 3), whose non trivial faces are defined by the following inequalities:

$$10S_{1} - 3S_{3} \leq 0,$$

$$30S_{1} - 8S_{2} - 3S_{3} \leq 0,$$

$$-10S_{1} + 4S_{2} + 3S_{3} \leq 60,$$

$$-5S_{1} + S_{2} + S_{3} \leq 15,$$

$$-2S_{1} + S_{3} \leq 8.$$

$$(66)$$

Although this reduced polytope contains \mathcal{S} , the exact shape of \mathcal{S} for N=6 remains unknown. The question of whether it is even a polytope remains open.

F. 7 and 8 qubits

We expect the set \mathcal{S} to exhibit a complex shape for N=7 and 8, similar to the case N=6. Indeed, we find that, while several optimal states for the sector lengths are achieved by \mathcal{R} (states in a grey cell in Table III), numerical searches reveal other states that produce tighter bounds for certain sector lengths. Therefore, additional conditions are needed to fully characterize \mathcal{S} .

V. SECTOR LENGTHS FOR ARBITRARY NUMBER OF QUBITS

In Sec. IV and Table III, we analyzed systems with a reduced number of qubits up to N=8. However, in certain cases, it is possible to derive explicit bounds for certain sector lengths that hold for arbitrary values of N. In the following, we present several examples of such bounds. Before proceeding with the proofs, we first calculate the sector lengths for both product states and GHZ states for an arbitrary number of qubits.

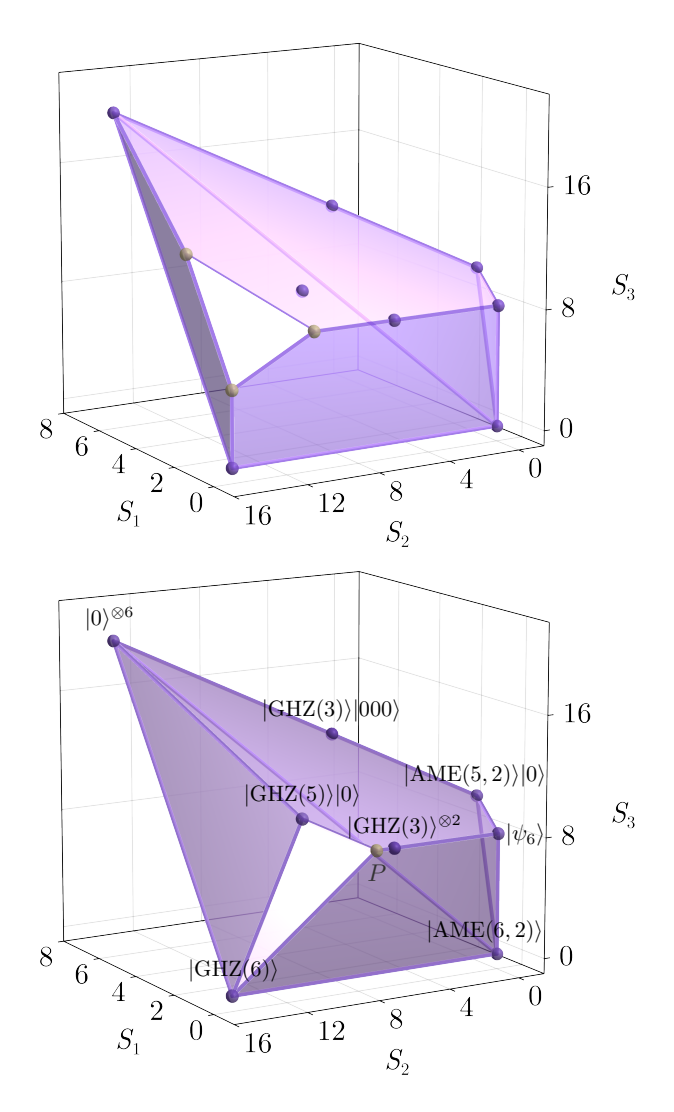


FIG. 3. Top: the polytope $\mathcal{R} = \mathcal{R}_2 \cap \mathcal{R}_3$ for N=6 in the (S_1, S_2, S_3) space. Bottom: smaller polytope obtained by including additional linear constraints given in Eq. (66), derived by numerical optimization. States corresponding to vertices or points along the edges are indicated. The vertex P=(0,7,8), shown in grey, is one for which we have not identified any state realizing these sector lengths.

A. Product and GHZ states

We start with product states. As sector lengths are SU(2) invariants, we can consider the state $|0\rangle^{\otimes N}$, for which we have

$$\langle \sigma_{\boldsymbol{\mu}} \rangle = \prod_{\alpha=1}^{N} \left(\delta_{0,\mu_{\alpha}} + \delta_{3,\mu_{\alpha}} \right). \tag{67}$$

Then, S_m is equal to the number of Pauli strings consisting of N-m 0 and m 3's, i.e.,

$$S_m(|0\rangle^{\otimes N}) = \binom{N}{m}.$$
 (68)

N	State	(S_1) or			
	20000	(S_1,S_2)			
	$ \mathrm{GHZ}(2)\rangle$	(0)	N	State	(S_1, S_2, S_3)
2	$ 0\rangle^{\otimes 2}$	(2)		$ AME(6,2)\rangle$	(0,0,0)
3	GHZ(3)⟩	(0)		$ \psi_6 angle$	(0, 0, 8)
	$ 0\rangle^{\otimes 3}$	(3)		$ \mathrm{GHZ}(6)\rangle$	(0, 15, 0)
			$\begin{vmatrix} 1 \\ 6 \end{vmatrix}$	$ 0\rangle^{\otimes 6}$	(6, 15, 20)
	tetra>	(0,2)	0	$ AME(5,2)\rangle 0\rangle$	(1,0,10)
4	$ GHZ(4)\rangle$	(0,6)		$ \mathrm{GHZ}(3)\rangle^{\otimes 2}$	(0, 6, 8)
	$ 0\rangle^{\otimes 4}$	(4,6)		$ GHZ(5)\rangle 0\rangle$	(1, 10, 10)
5	$ AME(5,2)\rangle$	(0,0)		$ \mathrm{GHZ}(3)\rangle 0\rangle^{\otimes 3}$	(3, 6, 14)
	$ \mathrm{GHZ}(5)\rangle$	(0, 10)			. , , ,
	$ 0\rangle^{\otimes 5}$	(5, 10)			

TABLE I. Sector lengths (S_1) , (S_1, S_2) and (S_1, S_2, S_3) for states associated with certain vertices of the polytope \mathcal{R} defined in Theorem 1. The last three states for N=6 correspond to points along the edges and were found to be extremal for some other sector length, see Table III. The states for N=4,5 and 6 are indicated in Figs. 1 and 3.

We now consider the $|\mathrm{GHZ}(N)\rangle$ state. The squared expectation value $|\langle \sigma_{\pmb{\mu}} \rangle|^2$ is equal to 1 if $\pmb{\mu}$ consists either of a vector of zeroes with an even number of 3's, or a vector of 1 with an even number of 2. In all other cases, this quantity vanishes. As a consequence, we find that $S_m = 0$ for all odd m < N. For even m < N, we have $S_m = \binom{N}{m}$, with nonzero contributions arising from Pauli strings of the form $\pmb{\mu} = \pmb{3}_m \pmb{0}_{N-m}$, up to permutations.

For the case m=N, the squared expectation value $|\langle \sigma_{\boldsymbol{\mu}} \rangle|^2$ equals 1 when $\boldsymbol{\mu}=\mathbf{1}_{N-j}\mathbf{2}_j$, with j ranging from 0 to N if N is even, or from 0 to N-1 if N is odd. These terms contribute a total of 2^{N-1} . In addition, for even N, there is one more nonzero contribution from the Pauli string $\boldsymbol{\mu}=\mathbf{3}_N$. Therefore, we find

$$S_N(|\text{GHZ}(N)\rangle) = \begin{cases} 2^{N-1} + 1 & \text{for } N \text{ even} \\ 2^{N-1} & \text{for } N \text{ odd} \end{cases} . \tag{69}$$

B. 1 and 2-body correlations

We found tight upper bounds for the sector lengths S_1 and S_2 that quantify the amount of 1 and 2-body correlations. The same bounds were also derived and formally proved in Ref. [5]. However, we observe here that these bounds follow straightforwardly from Eqs. (34)–(36).

First, consider Eqs. (34) and (35) with k=2

$${\binom{N}{2}S_0 + {\binom{N-1}{1}S_1 + {\binom{N-2}{0}S_2 \leqslant 4 \binom{N}{2}}, \\ -{\binom{N}{2}S_0 + {\binom{N-1}{1}S_1 - {\binom{N-2}{0}S_2 \leqslant 0}}.}$$
(70)

Subtracting the two equations, we obtain

$$S_1 \leqslant N. \tag{71}$$

Now, from Eq. (36) with k = 3, we obtain

$$\binom{N}{3}S_0 + \binom{N-2}{1}S_2 \leqslant 4\binom{N}{3}. \tag{72}$$

Since $S_0 = 1$ for any N, it follows that

$$S_2 \leqslant \binom{N}{2}.\tag{73}$$

One may conjecture from Eqs. (71) and (73) that the S_m are upper bounded by binomial coefficients $\binom{N}{m}$. This is no longer the case for S_3 , since for N=4 we have $S_3(|\text{tetra}\rangle)=8$, see Eq. (E2). The next subsection gives more general results on these upper bounds.

C. Upper bound for S_m with m > 2

The results presented in Table III show that the inequality $S_m \leq \binom{N}{m}$ holds for all multiqubit systems with $N \geq N_0$, where the minimal values are $N_0 = 2, 3, 5$ and 8 for m = 1, 2, 3 and 4, respectively. This property was previously established in Ref. [5], which states the following lemma:

Lemma 1 [5]. If $S_m(\rho) \leqslant \binom{N_0}{m}$ holds for all states ρ of N_0 qubits, then for any $N \geqslant N_0$, $S_m(\rho') \leqslant \binom{N}{m}$ holds for all N-qubit states ρ' .

In Lemma 1 states ρ and ρ' are not necessarily pure.

The key question is to determine whether such a minimal N_0 exists for each m, and to calculate the smallest N_0 such that $S_m(\rho) \leq \binom{N_0}{m}$ for all N_0 -qubit states ρ . This problem was posed as a conjecture to be proven in Ref. [5]. Using the lemma above, the conjecture can be restated as follows:

Conjecture 2 [5]. For every m, there exists an N_0 such that $S_m \leq \binom{N_0}{m}$ holds for all N_0 -qubit states. Consequently, according to Lemma 1, the inequality extends to all $N \geq N_0$.

Our findings in Sec. IV confirm this conjecture for m up to 5. For m=1,2, and 3, we find the same minimal N_0 as reported in Ref. [5]. The analytical maximization of S_m under the constraints defining \mathcal{R} (see Eq. (38)) establishes the conjecture for m=4 with $N_0=9$ and m=5 with $N_0=12$. However, the numerical data in Table III indicate that for m=4, the minimal N_0 might instead be 8.

D. Upper bound for S_N

The lower bound of S_N for an N-qubit system is 1, and this bound is saturated by product states, as shown

in Ref. [4]. The same reference proves that $S_N \leq 2^{N-1}$ for odd N, and conjectures that $S_N \leq 2^{N-1} + 1$ for even N. In both cases, the $|\mathrm{GHZ}(N)\rangle$ states saturate the inequality. This conjecture has been rigorously proved in Ref. [51], leading to the following Theorem

Theorem 2 [4, 51] For an N-qubit pure state, the sector length S_N has a minimum value of 1. Its maximum value is

$$\max S_N = \begin{cases} 2^{N-1}, & \text{if } N \text{ is odd,} \\ 2^{N-1} + 1, & \text{if } N \text{ is even.} \end{cases}$$

The minimum and maximum are attained by product states and GHZ states, respectively.

Here, we give an alternative proof of this result. Our strategy is the following: find an upper bound for S_N within some polytope containing S, and then show that this upper bound is reached within S, i.e. saturated by some quantum state.

Finding an upper bound for S_N under the constraint that the vector \mathbf{S} belongs to a polytope is a typical linear programming problem. In our case, we observed numerically that the maximum of S_N is reached when optimizing only under the constraints (16) for $1 \leq k \leq N/2$ and (36) for odd k. The linear programming problem in the variables $S_1, ..., S_N$ can be expressed as follows:

- find $\max(S_N)$
- under the constraints $S_m \ge 0, m = 1, ..., N$
- with inequality constraints for q = 1, ..., N/2 1

$$\sum_{m=1}^{q} {N-2m \choose 2q+1-2m} S_{2m} \leqslant (2^{2q}-1) {N \choose 2q+1}, \qquad (74)$$

corresponding to (36) for k = 2q + 1,

• and equality constraints for k = 0, ..., N/2 - 1

$$\frac{1}{2^{N-k}} \sum_{m=1}^{N-k} {\binom{N-m}{k}} S_m - \frac{1}{2^k} \sum_{m=1}^k {\binom{N-m}{N-k}} S_m = \left(\frac{1}{2^k} - \frac{1}{2^{N-k}}\right) {\binom{N}{k}}.$$
(75)

This linear problem takes the form of a primal problem over the variables S_m [54]:

- find $\max(\sum_{m} c_m S_m)$
- under the constraints $S_m \ge 0, m = 1, ..., N$,
- with $\sum_m a_{qm} S_m \leqslant b_q$ for q = 1, ..., N/2 1
- and $\sum_{m} a'_{km} S_m = b'_k$ for k = 0, ..., N/2 1,

with

$$c_{m} = \delta_{m,N}$$

$$a_{qm} = \binom{N-m}{2q+1-m} \delta_{m \text{ even}}$$

$$a'_{km} = \frac{1}{2^{N-k}} \binom{N-m}{k} - \frac{1}{2^{k}} \binom{N-m}{N-k}$$

$$b_{q} = (2^{2q} - 1) \binom{N}{2q+1}$$

$$b'_{k} = (\frac{1}{2^{k}} - \frac{1}{2^{N-k}}) \binom{N}{k}.$$
(76)

To this primal problem corresponds the following dual problem over the variables y_q, y'_k , corresponding to constraints (75) and (74), respectively:

- find min $\left(\sum_{q} b_q y_q + \sum_{k} b'_k y'_k\right)$
- under the constraints $y_q \ge 0$, q = 1, ..., N/2 1,
- and inequality constraints for m = 1, ..., N

$$\sum_{q=1}^{N/2-1} a_{qm} y_q + \sum_{k=0}^{N/2-1} a'_{km} y'_k \geqslant c_m.$$
 (77)

The constraints defining the primal problem are a subset of the constraints defining $\mathcal{R} \supset \mathcal{S}$. Therefore, all points in \mathcal{S} are feasible points of the primal problem and, by virtue of the weak duality theorem of linear programming, provide a lower bound for the dual problem. This is the case of the state $|\mathrm{GHZ}(N)\rangle$, for which Eq. (69) gives $S_N = 2^{N-1} + 1$. From the strong duality theorem, to conclude the proof, it suffices to show that there are feasible values of y_q, y_k' which achieve that lower bound.

We take the following values:

$$y_{q} = 0 1 \leqslant q \leqslant \frac{N}{4} - 1$$

$$y_{q} = 2^{1-N/2} q = \frac{N-2}{4} \text{ if } N \text{ mod } 4 = 2$$

$$y_{q} = 2^{-2q+1} \lfloor \frac{N+2}{4} \rfloor \leqslant q \leqslant \frac{N}{2} - 1 (78)$$

$$y'_{0} = 2^{N}$$

$$y'_{k} = \frac{2^{N-k} - 2^{k} + 1}{(-1)^{k}} - 1, 1 \leqslant k \leqslant \frac{N}{2} - 1.$$

The values (78) obviously follow the trivial constraints $y_q \ge 0$. As for the other inequality constraints, the left-hand side of Eq. (77) reads

$$Q_m = \sum_{q=1}^{N/2-1} a_{qm} y_q + \sum_{k=0}^{N/2-1} a'_{km} y'_k.$$
 (79)

In Appendix F1 we show that $Q_m \ge c_m$, which shows that the values (78) yield a feasible point for the dual problem. We show in Appendix F2 that at this point we have

$$\sum_{q=1}^{N/2-1} b_q y_q + \sum_{k=0}^{N/2-1} b_k' y_k' = 2^{N-1} + 1, \tag{80}$$

and thus $2^{N-1}+1$ is an upper bound of the primal problem. This proves that $S_N \leq 2^{N-1}+1$ for any pure state, with equality for the $|\mathrm{GHZ}(N)\rangle$ state.

VI. APPLICATIONS

Sector lengths can be used to define entanglement measures for pure states in the form of generalized multipartite concurrences (see Appendix D for more details on this relationship). In this section, we explore several applications of sector lengths related to these multipartite concurrences and to quantum coding theory.

A. Linear entropy of entanglement and shadow enumerators

Sector lengths are directly related to the linear entropy of entanglement of a pure state across a bipartition $A|\bar{A}$, defined as

$$E_L^A(\rho) \equiv 2 \left[1 - \text{Tr} \left(\rho_A^2 \right) \right].$$
 (81)

Using Eqs. (29) and (30), the average linear entropy of entanglement over all bipartitions of k and N-k qubits, $\overline{E}_L^k(\rho) \equiv \sum_{|A|=k} E_L^A(\rho)$, is indeed equal to

$$\overline{E}_L^k(\rho) = 2\binom{N}{k} \left[1 - \frac{1}{2^k} \sum_{m=0}^k \frac{\binom{k}{m}}{\binom{N}{m}} S_m(\rho) \right]. \tag{82}$$

The quantity $\overline{E}_L^k(\rho)$ vanishes if and only if the state is a product state. This is because $\overline{E}_L^k(\rho)$ is a positive linear combination of entanglement measures. Hence, $\overline{E}_L^k=0$ implies that the state is separable across all bipartitions $A|\overline{A}$ with |A|=k, which is equivalent to being a product state. On the other hand, for a k-uniform state, that is, a state that is maximally entangled across every bipartition with up to k qubits in subsystem A, it holds that

$$x_{\boldsymbol{\mu}_m \mathbf{0}_{N-m}} = \delta_{\boldsymbol{\mu}_m \mathbf{0}_m} \tag{83}$$

for any m-index vector μ_m . This is equivalent to

$$S_m = 0 \quad \forall \, m \leqslant k. \tag{84}$$

Such k-uniform states can exist only for $k \leq \lfloor N/2 \rfloor$. When $k = \lfloor N/2 \rfloor$, they are known as absolutely maximally entangled (AME) states and denoted by $|\mathrm{AME}(N,2)\rangle$ [17, 30], where the number 2 is related with the dimension of each subsystem. Thus, the maximum possible average linear entropy of entanglement is attained only by k-uniform states.

Other relevant quantities for quantifying entanglement are the shadow enumerators $S_g^{(e)}$, which are linear combinations of sector lengths (see Eq. (17)). These quantities have recently been used in the experimental characterization of entanglement [29]. As we demonstrate in Appendix D, they can also be interpreted as multipartite generalizations of concurrence. Furthermore, as shown in Appendix C, each shadow enumerator corresponds to the expectation value of a projector operator

acting in the double-copy Hilbert space. For pure states, the shadow enumerators satisfy $S_g^{(e)}(\rho) = 0$ for g - N odd and $\sum_{g=0}^{N} S_g^{(e)} = 2^N$ (see Appendix C).

For $N \leqslant 5$, we showed in Sec. V that the numerical range \mathcal{S} forms a polytope. It follows that the extremal values of any physical quantity expressed as a linear combination of S_m are reached by quantum states necessarily associated with the vertices of this polytope. More generally, the maximum or minimum of any monotonic function of such a linear combination will be reached at one of the vertices of the polytope¹. As a concrete example, for N=4 and N=5, the quantities \overline{E}_L^g and $S_g^{(e)}$ with g < N can be extremized by evaluating them over the finite set of extremal states from Table I, with the corresponding maximizers and minimizers summarized in Table II (including results for N=6, when available).

As discussed above, product states minimize \overline{E}_L^k , while for N=5 and 6, this quantity is maximized by AME states. For N=4, however, an $|\mathrm{AME}(4,2)\rangle$ state does not exist. In this case, the state $|\mathrm{tetra}\rangle$ maximizes \overline{E}_L^2 ; further details about this state can be found in Appendix E.

For N=4, the shadow enumerators (17) give

$$S_0^{(e)} = \frac{1}{4} (-2 - S_1 + S_2), \quad S_2^{(e)} = \frac{1}{2} (18 - 3S_1 - S_2),$$
(85)

and for N=5

$$S_1^{(e)} = \frac{1}{2} \left(-2S_1 + S_2 \right), \quad S_3^{(e)} = -2S_1 - S_2 + 20.$$
 (86)

Note that $S_3^{(e)}$ is maximized not only by $|\text{AME}(5,2)\rangle$ states, but also by the 5-qubit GHZ state, and that shadow enumerators are not always minimized by product states.

For $N \geqslant 6$, our results are not sufficient a priori to completely characterize the structure of \mathcal{S} ; however, we can search for extrema over the larger set \mathcal{R} . Since $\mathcal{S} \subset \mathcal{R}$, if an extremum is reached at a vertex of \mathcal{R} that corresponds to a realizable quantum state, then that state is guaranteed to be optimal. We apply this approach for N=6 to both the average linear entanglement entropy and the shadow enumerators. The linearly independent shadow enumerators in this case are

$$S_0^{(e)} = \frac{1}{8} (8 + 2S_1 - S_3),$$

$$S_2^{(e)} = \frac{1}{8} (-30S_1 + 8S_2 + 3S_3),$$

$$S_4^{(e)} = \frac{1}{8} (360 - 10S_1 - 16S_2 - 3S_3).$$
(87)

N	State	Minimum	Maximum	
	tetra>	$S_0^{(e)}$	$\overline{E}_L^1, \overline{E}_L^2, S_2^{(e)}$	
4	$ \mathrm{GHZ}(4)\rangle$		$\overline{E}_L^1, S_0^{(e)}$	
	$ 0\rangle^{\otimes 4}$	$\overline{E}_L^1, \overline{E}_L^2, S_0^{(e)}, S_2^{(e)}$		
	$ \mathrm{AME}(5,2)\rangle$	$S_1^{(e)}$	$\overline{E}_L^1, \overline{E}_L^2, S_3^{(e)}$	
5	$ GHZ(5)\rangle$		$\overline{E}_L^1, S_1^{(e)}$	
	$ 0\rangle^{\otimes 5}$	$\overline{E}_L^1, \overline{E}_L^2, S_1^{(e)}, S_3^{(e)}$		
		a(e)	$\overline{E}_L^1, \overline{E}_L^2, \overline{E}_L^3$	
	$ \mathrm{AME}(6,2)\rangle$	$S_2^{(e)}$	$S_0^{(e)}, S_4^{(e)}$	
	$ \psi_6\rangle^{(\mathrm{E}10)}$	$S_0^{(e)}$	$\overline{E}_L^1, \overline{E}_L^2$	
	$ GHZ(6)\rangle$		$\overline{E}_L^1, S_0^{(e)}, S_2^{(e)_{\mathbf{a}}}$	
6	$ 0\rangle^{\otimes 6}$	$\overline{E}_L^1, \overline{E}_L^2, \overline{E}_L^3$		
	107	$S_0^{(e)}, S_2^{(e)}, S_4^{(e)}$		
	$ AME(5,2)\rangle 0\rangle$	$S_0^{(e)}, S_2^{(e)}$		
	$ \mathrm{GHZ}(3)\rangle^{\otimes 2}$	$S_0^{(e)}$	\overline{E}_L^1	
	$ \mathrm{GHZ}(5)\rangle 0\rangle$	$S_0^{(e)}$		
	$ \mathrm{GHZ}(3)\rangle 0\rangle^{\otimes 3}$	$S_0^{(e)}, S_2^{(e)}$		
		(e)		

^a The optimality of $|{\rm GHZ}(6)\rangle$ for $S_2^{(e)}$ relies only on a global numerical optimization over the pure states space, not on our inequalities.

TABLE II. States lying on the boundary of the polytope \mathcal{R} and quantities they extremize among the average linear entanglement entropy and the shadow enumerators, \overline{E}_L^g and $S_g^{(e)}$, respectively.

We find that product states minimize all three shadow enumerators, though some of these minima are also attained by other states. The state $|\mathrm{AME}(6,2)\rangle$ is found to maximize both $S_0^{(e)}$ and $S_4^{(e)}$. Additionally, using our inequalities, we can analytically confirm that $|\mathrm{GHZ}(6)\rangle$ maximizes $S_0^{(e)}$. Numerical results further suggest that it also maximizes $S_2^{(e)}$, although this cannot be concluded from our inequalities alone.

B. The overlap R_{ρ}

Since the quantity $\text{Tr}(\rho_A^2) + R_{\rho_A}$ played a central role in deriving our inequalities for the sector lengths, we now examine its extremal values. In particular, we investigate whether the bounds given in Eq. (28) are saturated. Without loss of generality, we consider a bipartition $A|\bar{A}$, where A consists of the first k qubits. The case k=1 is a bit special because the Hilbert space of A is two-dimensional. In this setting, any orthonormal basis $\{|\phi_1\rangle, |\phi_2\rangle\}$ must satisfy $|\phi_2\rangle \propto |\tilde{\phi}_1\rangle$, since the orthogonal complement of $|\phi_1\rangle$ is one-dimensional, and for an odd number of qubits, $\langle \phi_1|\tilde{\phi}_1\rangle = 0$ (see Subsection II B).

¹ If the optimum is reached at several vertices, the complete extremal set corresponds to the convex hull of these vertices in the space S_m .

As a result, using Eq. (27), we find that for |A| = 1,

$$\operatorname{Tr}(\rho_A^2) + R_{\rho_A} = 1, \tag{88}$$

which we also found numerically for small values of N (see Table IV).

For k=|A|>1, the upper bound of $\operatorname{Tr}(\rho_A^2)+R_{\rho_A}$ depends on the parity of k. When k is odd, the bound is attained by product states with $\operatorname{Tr}(\rho_A^2)=1$ and $R_{\rho_A}=0$. For even k, the maximum is achieved by a state of the form $|\psi_A\rangle\otimes|0\rangle^{\otimes N_B}$, where $|\psi_A\rangle$ satisfies $|\tilde{\psi}_A\rangle\otimes|\psi_A\rangle$. An example is the Dicke state $|D_k^{(k/2)}\rangle$ defined in Eq. (E1), for which $\operatorname{Tr}(\rho_A^2)=1$ and $R_{\rho_A}=1$. This maximum value can be interpreted as a compromise between the purity of the reduced state ρ_A and the overlap R_{ρ_A} , when the sum is optimized.

For the minimum of $\operatorname{Tr}(\rho_A^2) + R_{\rho_A}$, Table IV lists examples of optimal states obtained numerically for systems with up to N=10 qubits and various values of k. The lower bound given in Eq. (28) is saturated when $N_A > N_{\bar{A}}$, i.e., when 2k > N. For $k \leq N-k$ and $k \neq 1$, numerical results consistently yield a minimum of 2^{-k+1} . It should be noted that the case N=10 with k=5 provides the first example in which the contributions of $\operatorname{Tr}(\rho_A^2)$ and R_{ρ_A} are neither completely balanced nor entirely concentrated in a single term. All these observations can be summarised in the following conjecture:

Conjecture 3 Let $A|\bar{A}$ be a bipartition of an N-qubit system into k=|A| and $N-k=|\bar{A}|$ qubits. Then, the minimum of $\mathrm{Tr}(\rho_A^2)+R_{\rho_A}$ taken over all pure states $|\psi\rangle$ of the N-qubit system, is given by

$$\min_{|\psi\rangle} \left(\text{Tr}(\rho_A^2) + R_{\rho_A} \right) = \begin{cases} 2^{k-N}, & \text{if } 2k > N, \\ 2^{-k+1}, & \text{if } 2k \leqslant N. \end{cases}$$
(89)

C. Quantum coding theory

Let us now discuss the connection between our results and quantum-error correction. For completeness, we briefly summarize key concepts of quantum error-correcting codes (QECCs) in the context of sector lengths restricted to qubits, following the references [22, 25]. Any error operator can be expressed as a linear combination of local error operators, which are simply Pauli strings σ_{μ} . Consequently, we focus on errors of the form $E = \sigma_{\mu}$.

A quantum code Q of dimension K is a vector subspace of the Hilbert space of N qubits, $(\mathbb{C}^2)^{\otimes N}$. An error operator E is said to be detectable by Q if

$$\langle \psi | E | \psi \rangle = c(E)$$
 for all $| \psi \rangle \in \mathcal{Q}$.

where c(E) is a constant depending only on E.

A quantum code \mathcal{Q} for qubits, specified by the triple ((N,K,d)), is a subspace of dimension K that detects all local errors with $\operatorname{wt}(\sigma_{\mu}) < d$. Such a code is referred to as a ((N,K,d)) QECC. The code is called *pure* if, for

any local error E, the expectation value satisfies $c(E) = 2^{-N} \text{Tr}(E)$. In our context, we focus on a single pure state, corresponding to a one-dimensional subspace (K = 1). QECCs of the form ((N, 1, d)) are known as *self-dual* codes and are, by convention, always considered pure. This basic theory allows us to highlight a link between QECCs and sector lengths.

Proposition 1 [22, 25]: A pure state $|\psi\rangle$ of N qubits has $S_m = 0$ if and only if it defines a (pure) ((N, 1, m + 1)) QECC.

In quantum coding theory, a more quantitative way to determine whether a code detects local errors of weight m is through the Shor-Laflamme enumerators, which are defined in terms of the projector $M_{\mathcal{Q}}$ on the code subspace \mathcal{Q} by [21, 27]

$$A_{m}(M_{\mathcal{Q}}, M_{\mathcal{Q}}) \equiv \sum_{\text{wt}(\sigma_{\mu})=m} \text{Tr} (\sigma_{\mu} M_{\mathcal{Q}})^{2},$$

$$B_{m}(M_{\mathcal{Q}}, M_{\mathcal{Q}}) \equiv \sum_{\text{wt}(\sigma_{\mu})=m} \text{Tr} (\sigma_{\mu} M_{\mathcal{Q}} \sigma_{\mu} M_{\mathcal{Q}}),$$
(90)

for $m=1,\ldots,N$. In the special case where K=1 (i.e., the code consists of a single state), the projector becomes $M_{\mathcal{Q}}=\rho=|\psi\rangle\langle\psi|$. In this case, the Shor-Laflamme enumerators reduce to the sector lengths: $A_m(\rho,\rho)=B_m(\rho,\rho)=S_m(\rho)$. For completeness, we present this result along with the more general framework of Shor-Laflamme enumerators [21] and their connection to sector lengths in Appendix B. We also discuss their relation to the MacWilliams identity and shadow inequalities.

VII. CONCLUSIONS

In this work, we studied the set S of admissible sector lengths $\mathbf{S} = (S_1, \dots, S_N)$ for pure N-qubit states. By combining known constraints on multipartite quantum correlations with the monogamy inequalities derived in this work, we constructed a polytope $\mathcal R$ containing $\mathcal S$ (see Theorem 1). For $N \leq 5$ qubits, we showed that this polytope precisely defines the boundary of \mathcal{S} . The states corresponding to the edges of \mathcal{R} were identified. and those corresponding to the vertices are listed in Table I. Extending our analysis to 6-qubit systems revealed a significant increase in complexity, with numerical evidence suggesting that $\mathcal{R} \neq \mathcal{S}$ in this case. The origin of additional constraints on sector lengths defining \mathcal{S} for $N \geqslant 6$ remains to be determined, as does the more general question of whether the set \mathcal{S} continues to form a polytope for larger N.

We also systematically identified, numerically or analytically, pure states that extremize sector lengths S_m (i.e., lie on the boundary of S) for all m for $N \leq 8$. These states, listed in Table III, include known exceptional states as well as previously unknown states. Those highlighted in gray have been analytically verified as optimal by saturating inequalities defining $\mathcal{R} \supset S$. Our

inequalities also provided an alternative proof for a conjecture on the maximum value of S_N (see Theorem 2) from Ref. [4], and validated Conjecture 2 from Ref. [5] for S_4 with $N_0 \leq 9$ and for S_5 for $N_0 \leq 12$.

The search for new monogamy inequalities is essential to refine the geometric understanding of the set S. To this end, we examined the sum of the purity and the overlap of the reduced states, $Tr(\rho_A^2) + R_{\rho_A}$, and found that some extremal states do not saturate our bounds (see Conjecture 3), suggesting that there is still potential to find further and sharper inequalities. A complete characterization of the set S is valuable for identifying states that optimize physical quantities expressible only in terms of sector lengths. When such a quantity is a monotonic function of a linear combination of S_m , the search space reduces to the boundary of S, or if S is a polytope, its vertices. Leveraging this, we determined states extremizing the average linear entropy of entanglement and the quantum shadow enumerators for N=4,5and 6 (see Table II). Both quantities, which are examples of generalized concurrences, depend linearly on sector lengths. Additionally, we showed that the shadow enumerators can be interpreted as the expectation value of a projector in the double-copy Hilbert space.

In summary, our results once again highlight the complex structure of multipartite quantum correlations, with a notable increase in complexity at N=6, suggesting the existence of stricter constraints that remain to be found. The extremal states identified here could constitute key resources in the fields of quantum entanglement and quantum information, motivating further studies on their properties and potential generalizations.

ACKNOWLEDGEMENTS

ESE acknowledges support from the postdoctoral fellowship of the IPD-STEMA program of the University of Liège (Belgium). JM and ESE acknowledge the FWO and the F.R.S.-FNRS for their funding as part of the Excellence of Science programme (EOS project 40007526). OG thanks T. Paterek for useful discussion.

Appendix A: Derivation of Eqs. (16) and (30)

Let us first prove Eq. (30). We start by considering the simplest case, when subsystem A contains k=3 qubits.

1. Case k=3

Consider a 3-qubit mixed state ρ_A . If ρ_A is the reduced state of a larger pure quantum state of N qubits, its coordinates correspond to the variables x_{μ} , where the multi-indices μ have at least N-3 zeros (see Eqs. (2)–(3)). For example, if subsystem A corresponds to the three first qubits, its variables are the $x_{\mu_1\mu_2\mu_3}\mathbf{0}_{N-3}$ of

the original pure state of the N-qubit system. We now calculate the sector length S_1 of ρ_A , which is

$$S_1(\rho_A) = \sum_{a=1}^3 \left(x_{a00\mathbf{0}_{N-3}}^2 + x_{0a0\mathbf{0}_{N-3}}^2 + x_{00a\mathbf{0}_{N-3}}^2 \right). \tag{A1}$$

Summing over all $\binom{N}{k}$ bipartitions $A|\bar{A}$, where \bar{A} is the complementary subset of A, each $x^2_{a00}\mathbf{0}_{N-3}$ appears in all triplets involving the first qubit, that is, $\binom{N-1}{2}$ times. Therefore

$$\sum_{|A|=k} S_1(\rho_A)$$

$$= {N-1 \choose 2} \sum_{a=1}^3 \left(x_{a00...0}^2 + x_{0a0...0}^2 + ... + x_{0...0a}^2 \right) \quad (A2)$$

$$= {N-1 \choose 2} S_1(\psi).$$

Similarly,

$$S_2(\rho_A) = \sum_{a,b=1}^{3} \left(x_{ab0}^2 \mathbf{0}_{N-3} + x_{a0b}^2 \mathbf{0}_{N-3} + x_{0ab}^2 \mathbf{0}_{N-3} \right)$$
(A3)

and each $x_{ab0}^2 \mathbf{0}_{N-3}$ appears $\binom{N-2}{1} = N-2$ times in the sum over A, thus

$$\sum_{|A|=k} S_2(\rho_A)$$

$$= (N-2) \sum_{a,b=1}^3 \left(x_{ab0...0}^2 + x_{a0b0...0}^2 + \dots + x_{0...0ab}^2 \right)$$

$$= {\binom{N-2}{1}} S_2(\psi). \tag{A4}$$

2. General k

Equations (A2) and (A4) are easily generalized to arbitrary values of k. If A corresponds to the k first qubits, $S_m(\rho_A)$ with $m \leq k$ is given by

$$S_m(\rho_A) = \sum_{a_1,\dots,a_m=1}^3 \left(x_{a_1 a_2 \dots a_m 0 \dots 0}^2 \mathbf{0}_{N-k} + \dots + x_{00 a_1 a_2 \dots a_m}^2 \mathbf{0}_{N-k} \right). \quad (A5)$$

We then sum over all $\binom{N}{k}$ bipartitions $A|\bar{A}$, where A consists of k qubits. Each term $x_{a_1a_2...a_m}^2\mathbf{0}_{N-m}\mathbf{0}_{N-k}$ appears in every k-qubit subsystem that includes the first m qubits, which occurs $\binom{N-m}{k-m}$ times. However, it appears only once in $S_m(\psi)$. This is true for all terms in Eq. (A5), which leads to Eq. (30) for $m \leq k$.

Equation (16) is then obtained by expressing the purity of the reduced state ρ_A as

$$\operatorname{Tr}(\rho_A^2) = \frac{1}{2^k} \sum_{m=1}^k S_m(\rho_A).$$
 (A6)

Combining this with Eq. (30), we obtain

$$\sum_{|A|=k} \operatorname{Tr}\left(\rho_A^2\right) = \frac{1}{2^k} \sum_{m=1}^k {N-m \choose k-m} S_m(\psi). \tag{A7}$$

Since $\mathrm{Tr}(\rho_A^2)=\mathrm{Tr}(\rho_{\bar{A}}^2)$ holds for any pure state, we have that

$$\sum_{|A|=k} \operatorname{Tr}\left(\rho_A^2\right) = \sum_{|\bar{A}|=k} \operatorname{Tr}\left(\rho_{\bar{A}}^2\right),\tag{A8}$$

which directly leads to Eq. (16).

Appendix B: Shor-Laflamme enumerators and sector lengths

We describe the connection between sector lengths and some concepts that appear in quantum coding theory [21, 27]. For any two Hermitian operators M_1 and M_2 , the Shor-Laftamme enumerators (or weights) are defined as²

$$A_{m}(M_{1}, M_{2}) \equiv \sum_{\text{wt}(\sigma_{\mu})=m} \text{Tr}(\sigma_{\mu}M_{1})\text{Tr}(\sigma_{\mu}M_{2}),$$

$$B_{m}(M_{1}, M_{2}) \equiv \sum_{\text{wt}(\sigma_{\mu})=m} \text{Tr}(\sigma_{\mu}M_{1}\sigma_{\mu}M_{2}).$$
(B1)

We define two-variable polynomials using these enumerators

$$A(x,y) = \sum_{0 \le i \le N} A_m(M_1, M_2) x^{N-m} y^m,$$
 (B2)

and analogously for B(x,y). Theorem 7 of Ref. [25] (first proved in Ref. [21]) establishes a duality relation between A(x,y) and B(x,y), namely

$$B(x,y) \equiv A\left(\frac{x+3y}{2}, \frac{x-y}{2}\right),$$

$$A(x,y) \equiv B\left(\frac{x+3y}{2}, \frac{x-y}{2}\right).$$
(B3)

These identities are the quantum analog of the $MacWilliams\ identities$ used in classical coding theory over GF(4) [55].

In Ref. [27], Rains introduced another enumerator inspired by classical shadow codes [56]. These quantum shadow enumerators, denoted by C_m , are given by

$$C_m(M_1, M_2) = B_m(M_1, \tilde{M}_2),$$
 (B4)

where $\tilde{M}_2 = \sigma_y^{\otimes N} M_2^* \sigma_y^{\otimes N}$, and M_2^* is the complex conjugation of M_2 . Moreover, the associated polynomial C(x,y) satisfies [27]

$$C(x,y) = A\left(\frac{x+3y}{2}, \frac{y-x}{2}\right).$$
 (B5)

Theorem 10 of Ref. [27] shows that

$$C_m = \frac{1}{2^N} \sum_{i=0}^{N} (-1)^i K_m(i, N) A_i \geqslant 0.$$
 (B6)

The inverse relation of Eq. (B6) is given by

$$\sum_{i=0}^{N} K_m(i,N)C_i = \frac{1}{2^N} \sum_{i,j=0}^{N} (-1)^j K_m(i,N)K_i(j,N)A_j$$
$$= 2^N (-1)^m A_m,$$
(B7)

where the second equality follows from the orthogonality relation of the Kravchuk polynomials (Corollary 2.3 in Ref. [50])

$$\sum_{i=0}^{N} K_{m'}(i, N) K_i(m, N) = 4^N \delta_{m, m'}.$$
 (B8)

We now establish the connections between the Shor-Laflamme enumerators, the sector lengths S_m , and the shadow enumerators $S^{(e)}$ for quantum states. For $M_1 = M_2 = \rho$, we have that $A_m(\rho, \rho) = S_m(\rho)$ and $C_m(\rho, \rho) = S_m^{(e)}(\rho)$, which leads to Eq. (17). If we use instead $M_1 = \rho = \tilde{M}_2$, we obtain the inequality

$$\frac{1}{2^N} \sum_{m=0}^{N} K_{m'}(m, N) \underbrace{A_m(\rho, \rho)}_{S_m(\rho)} \geqslant 0,$$
 (B9)

where we have used $A_m(M_1, M_2) = (-1)^m A_m(M_1, M_2)$ which follows from the properties of Pauli strings. Alternatively, we can use $M_1 = M_2 = \rho_A$ with ρ_A the k-qubit reduced state obtained after tracing over a subsystem \bar{A} . Thus, we obtain another family of inequalities

$$\frac{1}{2^k} \sum_{i=0}^k (-1)^i K_m(i,k) A_i(\rho_A, \rho_A) \geqslant 0.$$
 (B10)

Summing over all the partitions of the same size (as in Eqs. (A6) and (A7)) yields

$$\frac{1}{2^k} \sum_{i=0}^k (-1)^i K_m(i,k) {N-i \choose k-i} \underbrace{A_i(\rho,\rho)}_{S_i(\rho)} \geqslant 0.$$
 (B11)

Notably, numerical evidence shows us that the inequalities (B9) and (B11) are less restrictive than Eq. (17).

² We adopt the definition of the Shor-Laflamme enumerators from Ref. [27], which agrees with the original formulation up to a global factor [21].

Appendix C: Shadow inequalities from the double-copy Hilbert space

Here, we derive the shadow inequalities (17) that define \mathcal{R}_2 [see Eq. (23)]. For that purpose, we use the double-copy of the initial Hilbert space of N qubits, $\mathcal{H}_1^{\otimes N} \otimes \mathcal{H}_1^{\otimes N}$, where \mathcal{H}_1 is the Hilbert space of a single qubit. This double-copy technique has also been used to study the concurrence for mixed states in [9, 57, 58]. We start with a reformulation of the S_m variables

$$S_{m} = \sum_{\text{wt}(\sigma_{\mu})=m} |\langle \psi | \sigma_{\mu} | \psi \rangle|^{2}$$

$$= \langle \Psi | \left(\sum_{\text{wt}(\sigma_{\mu})=m} \sigma_{\mu} \otimes \sigma_{\mu} \right) |\Psi \rangle$$

$$= \langle \Psi | \hat{S}_{m} | \Psi \rangle,$$
(C1)

where $|\Psi\rangle = |\psi\rangle \otimes |\psi\rangle$ and the sum runs over the multiindices μ with m non-zero entries. Thus, the sector length S_m of a pure state $|\psi\rangle$ can be thought of as the expectation value of an observable \hat{S}_m ³. The terms of the operators \hat{S}_m are grouped as

$$\hat{S}_{m} = \sum_{\text{wt}(\sigma_{\mu})=m} \sigma_{\mu} \otimes \sigma_{\mu}$$

$$= \sum_{\pi \in \text{Sym}(N)} \sum_{a_{1},\dots a_{m}=1}^{3} \frac{\sigma_{\pi(a_{1},\dots a_{m}\mathbf{0}_{N-m})} \otimes \sigma_{\pi(a_{1},\dots a_{m}\mathbf{0}_{N-m})}}{m!(N-m)!},$$
(C2)

where $\operatorname{Sym}(N)$ is the permutation group of N elements, and the denominator accounts for multiplicities to ensure that each distinct term appears exactly once. The index a_{α} appears twice, in the positions α and $N+\alpha$, and sums from 1 to 3. To calculate the eigenspectrum of \hat{S}_m , we start with the decomposition

$$\sum_{a=1}^{3} (\sigma_{a})_{\alpha} \otimes (\sigma_{a})_{N+\alpha}$$

$$= \sum_{j=0}^{1} \sum_{m=-j}^{j} F(j) |j,m\rangle_{\alpha,N+\alpha} \langle j,m|_{\alpha,N+\alpha}$$

$$= F(1)\hat{\mathcal{P}}_{1}^{(\alpha)} + F(0)\hat{\mathcal{P}}_{0}^{(\alpha)}.$$
(C3)

where

$$F(j) \equiv 2j(j+1) - 3 = \begin{cases} 1 & j=1 \\ -3 & j=0 \end{cases},$$

$$\hat{\mathcal{P}}_{1}^{(\alpha)} \equiv \sum_{m=-1}^{1} |1, m\rangle_{\alpha, N+\alpha} \langle 1, m|_{\alpha, N+\alpha} ,$$

$$\hat{\mathcal{P}}_{0}^{(\alpha)} \equiv |0, 0\rangle_{\alpha, N+\alpha} \langle 0, 0|_{\alpha, N+\alpha} ,$$
(C4)

and $|j,m\rangle_{\alpha,N+\alpha}$ denotes the corresponding triplet and singlet states of the two coupled qubits formed by the α -th and $(N+\alpha)$ -th qubits.

Thus, the eigenvectors of \hat{S}_m are

$$\hat{S}_{m} \bigotimes_{\alpha=1}^{N} |j_{\alpha}, m_{\alpha}\rangle_{\alpha, N+\alpha}
= e_{m}(F(j_{1}), \dots, F(j_{N})) \bigotimes_{\alpha=1}^{N} |j_{\alpha}, m_{\alpha}\rangle_{\alpha, N+\alpha},$$
(C5)

where $e_m(x_1, \ldots, x_N)$ is the *m*-th elementary symmetric function of N variables

$$e_m(x_1, \dots, x_N) \equiv \sum_{1 \le j_1 \le j_2 < \dots < j_m \le N} x_{j_1} \dots x_{j_m}. \quad (C6)$$

We can observe that all the \hat{S}_m operators have common eigenvectors. Consequently, $[\hat{S}_m, \hat{S}_{m'}] = 0$. Also, each eigenvalue (C5) has degeneracy $\binom{g}{g} 3^g$ where g is equal to the number of j equal to 1. This implies that

$$\hat{S}_m = \sum_{g=0}^{N} \lambda_{m,g} \hat{\mathcal{Q}}_g, \tag{C7}$$

with

$$\lambda_{m,g} = e_m \left(\underbrace{F(1), \dots, F(1)}_{g}, \underbrace{F(0), \dots, F(0)}_{N-g} \right).$$

$$= e_m \left(\underbrace{1, \dots, 1}_{g}, \underbrace{-3, \dots, -3}_{N-g} \right)$$

$$= \sum_{s=0}^{m} {g \choose s} {N-g \choose m-s} (-3)^{m-s}$$

$$= (-1)^m K_m(g, N),$$
(C8)

where we have used the generating function of the symmetric polynomials [59], and the last expression are the Kravchuk polynomials (18). The \hat{Q}_g operators are given by

$$\hat{\mathcal{Q}}_g = \frac{1}{g!(N-g)!} \sum_{\pi \in \text{Sym}(N)} \left(\bigotimes_{i=1}^g \hat{\mathcal{P}}_1^{\pi(i)} \right) \otimes \left(\bigotimes_{i=g+1}^N \hat{\mathcal{P}}_0^{\pi(i)} \right). \tag{C9}$$

The state $|\Psi\rangle$ is symmetric under the swap operator $S_{12}(|\psi_1\rangle\otimes|\psi_2\rangle)=|\psi_2\rangle\otimes|\psi_1\rangle$. Over this permutation, $|j,m_j\rangle_{\alpha,N+\alpha}$ transforms to $(-1)^{j+1}|j,m_j\rangle_{\alpha,N+\alpha}$. Hence, $\hat{\mathcal{Q}}_q|\Psi\rangle=0$ whenever N-g is odd.

By denoting the expectation value of the projections $\langle \Psi | \hat{Q}_g | \Psi \rangle = Q_g$, we can write S_m as

$$S_m = \sum_{g=0}^{N} (-1)^m K_m(g, N) Q_g,$$
 (C10)

and $Q_g = 0$ for N - g odd. Notably, the Q_g coefficients are proportional to the shadow enumerators (20).

³ We can also make this generalization for mixed states, $S_m(\rho) = \text{Tr}[(\rho \otimes \rho)\hat{S}_m].$

To prove this, we use the orthogonality condition of the Kravchuk polynomials (B8) in the previous equation and in Eq. (20), which gives $S_g^{(e)} = 2^N Q_g$. Therefore, $S_g^{(e)} = 0$ for N-g odd. Additionally, since $\sum_{g=0}^N \hat{Q}_g$ is equal to the identity matrix in the symmetric sector of $\mathcal{H} \otimes \mathcal{H}$, then

$$\sum_{g=0}^{N} S_g^{(e)} = 2^N. (C11)$$

Consequently, there are only $\lfloor N/2 \rfloor$ linearly independent shadow enumerators.

Appendix D: Multipartite concurrences

Tensor products of the projectors $\hat{\mathcal{P}}_{x}^{(\alpha)}$ defined in Appendix C are used in Refs. [9, 57, 58] to define multipartite concurrences⁴. More specifically, a generalized multipartite concurrence $C_{\hat{\mathcal{A}}}(|\psi\rangle)$ with respect to $\hat{\mathcal{A}}$ is defined as

$$C_{\hat{\mathcal{A}}}(|\psi\rangle) = 2\sqrt{\langle \psi | \otimes \langle \psi | \hat{\mathcal{A}} | \psi \rangle \otimes |\psi\rangle}, \qquad (D1)$$

where

$$\hat{\mathcal{A}} = \sum_{s_1, \dots, s_N = 0}^{1} p_{s_1, \dots, s_N} \hat{\mathcal{P}}_{s_1}^{(1)} \otimes \dots \otimes \hat{\mathcal{P}}_{s_N}^{(N)}, \tag{D2}$$

with the $p_{s_1...s_N}$ coefficients such that

$$\langle \psi | \otimes \langle \psi | \hat{\mathcal{A}} | \psi \rangle \otimes | \psi \rangle \geqslant 0$$
 (D3)

for all $|\psi\rangle \in \mathcal{H}$ [58], i.e., $\hat{\mathcal{A}}$ is a positive semidefinite operator in the symmetric sector of $\mathcal{H} \otimes \mathcal{H}^5$. For example, the \hat{S}_m (Eq. (C7)) and $\hat{\mathcal{Q}}_g$ (Eq. (C9)) operators fulfill (D3). Therefore, the sector lengths S_m and the shadow enumerators $S_g^{(e)}$ are particular cases of multipartite concurrences. The quantity R_ρ in Eq. (11) which, for pure states, is equal to $S_0^{(e)}(\rho)$ (19), can thus be seen as a generalized concurrence [48, 60, 61]. Finally, note that these concurrences can also be generalized to mixed states via the convex-roof extension [58].

Appendix E: Optimal states

In this Appendix, we present analytical expressions for proven or putative optimal states that extremize certain sector lengths or $\text{Tr}(\rho_A^2) + R_{\rho_A}$. Most of these states

have been deduced from numerical optimization. Their extremality is then either rigorously established based on our inequalities and those existing in the literature, or supported by numerical optimization, see Tables III and IV for more details.

Before presenting the states, we recall that a k-uniform N-qubit state is one for which all the reduced density matrices of at most k qubits are maximally mixed. When $k = \lfloor N/2 \rfloor$, such states are known as $\mathrm{AME}(N,2)$. Consequently, for a k-uniform state, all sector lengths S_m vanish for $m \leq k$; that is, $S_m = 0$ for all $m \leq k$.

As some optimal states are symmetric, it is useful to express them in terms of symmetric N-qubit Dicke states

$$|D_N^{(\alpha)}\rangle = {N \choose \alpha}^{-1/2} \sum_{\pi} |\pi(\underbrace{00\dots 0}_{N-\alpha} \underbrace{11\dots 1}_{\alpha})\rangle,$$
 (E1)

where $\alpha=0,\ldots,N$, and the sum runs over all permutations π of the N qubit labels. Symmetric N-qubit states can be uniquely represented by configurations of Majorana points on the Bloch sphere, known as Majorana stellar constellation [62, 63]. In the following, certain state names explicitly refer to this geometric representation.

$$N = 4$$

• The symmetric 4-qubit tetrahedron state, given by

$$|\text{tetra}\rangle = \frac{1}{2} \left(|D_4^{(0)}\rangle + i\sqrt{2} |D_4^{(2)}\rangle + |D_4^{(4)}\rangle \right), \quad (E2)$$

minimizes both S_1 and S_2 and maximizes S_3 . It has sector lengths

$$\mathbf{S} = (0, 2, 8, 5). \tag{E3}$$

Among all symmetric four-qubit states, it stands out as the unique maximally entangled one [64–66]. Each of its two-qubit reduced density matrices is maximally mixed within the symmetric subspace, having non-zero eigenvalues $(\frac{1}{3}, \frac{1}{3}, \frac{1}{3})$. Its extremality has been established analytically.

$$N = 5$$

• The 2-uniform 5-qubit state [17, 33, 67]

$$|\text{AME}(5,2)\rangle = \frac{1}{\sqrt{8}} (|00000\rangle + |00011\rangle + |01101\rangle + |01110\rangle + |10101\rangle - |10110\rangle + |11000\rangle - |11011\rangle)$$
(F4)

minimizes both S_1 and S_2 and maximizes S_4 . It has sector lengths

$$\mathbf{S} = (0, 0, 10, 15, 6). \tag{E5}$$

All extremality properties have been established analytically.

⁴ In Ref. [58], the operator $\hat{\mathcal{P}}_{1}^{(\alpha)}$ ($\hat{\mathcal{P}}_{0}^{(\alpha)}$) is denoted by $P_{+}^{(\alpha)}$ ($P_{-}^{(\alpha)}$).

⁵ The positive semidefinite condition of $\hat{\mathcal{A}}$ over the symmetric sector of $\mathcal{H}\otimes\mathcal{H}$ holds, but not necessarily [58], when all the $p_{s_1,...,s_N}$ coefficients are positive.

• The state

$$|\psi_5\rangle = \frac{1}{\sqrt{8}} (|00000\rangle + |00011\rangle - |00101\rangle + |00110\rangle + |10000\rangle + |10011\rangle + |10101\rangle - |10110\rangle)$$
 (E6)

has sector lengths

$$\mathbf{S} = (1, 2, 10, 13, 5) \tag{E7}$$

and is used in the superposition (60) to cover part of the right boundary of \mathcal{R} .

$$N = 6$$

• The 2-uniform 6-qubit state [17, 33, 67]

$$\begin{split} |\mathrm{AME}(6,2)\rangle &= \tfrac{1}{5} \big(|000000\rangle + |000011\rangle + |000101\rangle \\ &+ |000110\rangle + |001001\rangle - |001010\rangle - |001100\rangle \\ &+ |001111\rangle + |010001\rangle + |010100\rangle - |010111\rangle \\ &+ |011000\rangle - |011011\rangle + |011101\rangle - |011111\rangle \\ &+ |010001\rangle - |100100\rangle + |100111\rangle + |101000\rangle \\ &+ |101011\rangle + |101110\rangle + |110000\rangle + |110011\rangle \\ &+ |110101\rangle + |111000\rangle \big) \end{split}$$

minimizes both S_1 and S_2 and maximizes S_4 . It has sector lengths

$$\mathbf{S} = (0, 0, 0, 45, 0, 18). \tag{E9}$$

Its extremal properties have been established analytically.

• The 2-uniform 6-qubit state

$$|\psi_{6}\rangle = \frac{1}{4} (|000000\rangle + |000111\rangle + |001110\rangle + |010101\rangle + |100100\rangle + |110001\rangle + |110110\rangle + |1111111\rangle - |001001\rangle - |010010\rangle - |011011\rangle - |011100\rangle - |100011\rangle - |101010\rangle - |101101\rangle - |111000\rangle) (E10$$

minimizes both S_1 and S_2 . It has 12 of its 3-qubit reduced density matrices maximally mixed. The remaining 8 have an identical spectrum $(0,0,0,0,\frac{1}{4},\frac{1}{4},\frac{1}{4},\frac{1}{4})$. The sector lengths for this state are

$$\mathbf{S} = (0, 0, 8, 21, 24, 10), \tag{E11}$$

corresponding to a vertex of the polytope shown in Fig. 3.

• The 1-uniform 6-qubit symmetric state⁶

$$|\text{pyramid}\rangle = -\frac{1}{2}|D_6^{(0)}\rangle + \frac{\sqrt{3}}{2}|D_6^{(4)}\rangle$$
 (E12)

minimizes S_1 and maximizes S_5 . It has sector lengths

$$\mathbf{S} = \left(0, \frac{27}{5}, 8, \frac{51}{5}, 24, \frac{77}{5}\right). \tag{E13}$$

Its extremal properties have been established analytically.

$$N = 7$$

• The 1-uniform 7-qubit symmetric state

$$|\psi_7\rangle = \mathcal{N}\left(2\sqrt{2}\,|D_7^{(0)}\rangle + \sqrt{14}\,|D_7^{(3)}\rangle + \sqrt{14}\,|D_7^{(6)}\rangle\right)$$
 (E14)

minimizes both S_1 and S_4 and maximizes S_6 . Its sector lengths are given by

$$\mathbf{S} = (0, 7, 14, 7, 28, 49, 22). \tag{E15}$$

All its two-qubit reduced states have non-zero eigenvalues $(\frac{1}{3}, \frac{1}{3}, \frac{1}{3})$, while its three-qubit reduced states have non-zero eigenvalues $(\frac{1}{10}, \frac{2}{10}, \frac{3}{10}, \frac{4}{10})$. Its extremality for S_4 and S_6 has not been established analytically but is supported by our numerical results.

⁶ Its name comes from its Majorana constellation consisting of a square pyramid (the top vertex is twice degenerate) whose base is at a polar angle $\theta = -2 \arctan(3^{1/4} 5^{1/8})$.

• The 2-uniform 7-qubit state given in Eq. (17) of Ref. [68], which reads

$$|\psi_{M}\rangle_{1234567} = \frac{1}{4\sqrt{2}} \Big[|0000000\rangle + |0000011\rangle + |0001101\rangle + |0001110\rangle + |0010001\rangle - |0010010\rangle + |0011100\rangle - |0011111\rangle \\ - |0100101\rangle - |0100110\rangle + |0101000\rangle + |0101011\rangle + |0110100\rangle - |0110111\rangle - |0111001\rangle + |0111010\rangle \\ - |1000100\rangle - |1000111\rangle + |1001001\rangle + |1001010\rangle + |1010101\rangle - |1010110\rangle - |1011000\rangle + |1011011\rangle \\ + |1100001\rangle + |1100010\rangle + |1101100\rangle + |1101111\rangle + |1110000\rangle - |1110011\rangle + |1111110\rangle \Big].$$
(E16)

minimizes both S_1 and S_2 , which are both zero. This state has 32 of its 3-qubit reduced density matrices maximally mixed. The remaining three have the spectrum $(0,0,0,0,\frac{1}{4},\frac{1}{4},\frac{1}{4},\frac{1}{4})$. Its sector lengths are

$$\mathbf{S} = (0, 0, 3, 29, 42, 34, 19). \tag{E17}$$

• The 7-qubit state

$$|\psi_{7b}\rangle = \frac{1}{\sqrt{13}} \left[\sqrt{\frac{3}{2}} |0000\rangle \otimes (|001\rangle - |100\rangle) + |0001010\rangle + |0101000\rangle + |0110000\rangle + |0011000\rangle + |0110000\rangle + |011000\rangle + |0110$$

with $\omega = e^{i\pi/3}$, maximizes S_5 and has sector lengths

$$\mathbf{S} = \left(\frac{25}{13}, \frac{9}{13}, \frac{125}{13}, 35, \frac{603}{13}, \frac{355}{13}, \frac{79}{13}\right). \tag{E19}$$

Its extremality has not been established analytically but is supported by our numerics.

$$N = 8$$

• The 3-uniform 8-qubit state given in Eq. (19) of Ref. [69], which reads

$$|\psi_{M}\rangle_{12783456} = \frac{1}{8} \Big[\Big(|0000\rangle + |0011\rangle - |1101\rangle + |1110\rangle \Big)_{1278} \otimes \Big(|0000\rangle + |0111\rangle - |1001\rangle + |1110\rangle \Big)_{3456}$$

$$+ \Big(- |0001\rangle + |0010\rangle + |1100\rangle + |1111\rangle \Big)_{1278} \otimes \Big(|0001\rangle + |0110\rangle + |1000\rangle - |1111\rangle \Big)_{3456}$$

$$+ \Big(|0100\rangle - |0111\rangle + |1001\rangle + |1010\rangle \Big)_{1278} \otimes \Big(- |0011\rangle + |0100\rangle + |1010\rangle + |1101\rangle \Big)_{3456}$$

$$+ \Big(|0101\rangle + |0110\rangle + |1000\rangle - |1011\rangle \Big)_{1278} \otimes \Big(- |0010\rangle + |0101\rangle - |1011\rangle - |1100\rangle \Big)_{3456} \Big],$$
(E20)

where the multi-indices denote the qubit labels, minimizes both S_1, S_2 and S_3 , which are all zero. Its sector lengths are given by

$$\mathbf{S} = (0, 0, 0, 26, 64, 72, 64, 29). \tag{E21}$$

 \bullet The 2-uniform 8-qubit symmetric state

$$|\text{tetra}(8)\rangle = \frac{1}{3\sqrt{3}} \left(\sqrt{7} |D_8^{(0)}\rangle + 2 |D_8^{(3)}\rangle + 4 |D_8^{(6)}\rangle \right)$$
 (E22)

minimizes both S_1 and S_2 and maximizes S_7 . This state has doubly degenerate Majorana stars at the vertices of a tetrahedron. Its sector lengths are given by

$$\mathbf{S} = (0, 0, 3, 29, 42, 34, 19). \tag{E23}$$

Its extremality for S_7 has not been established analytically but is supported by our numerics.

• The 8-qubit state $|\text{tetra}\rangle^{\otimes 2}$ with $|\text{tetra}\rangle$ given in Eq. (E2) minimizes S_1 and S_4 and has sector lengths

$$\mathbf{S} = (0, 4, 16, 14, 32, 84, 80, 25). \tag{E24}$$

Its extremality for S_4 has not been established analytically but is supported by our numerics.

• The 3-uniform 8-qubit state given in Eq. (12) of Ref. [70], which reads

$$\begin{split} |\psi^{1}_{12345678}\rangle &= \frac{1}{4\sqrt{2}} \Big[\Big(|0000\rangle + |1111\rangle \Big)_{1256} \otimes \Big(|0000\rangle + |0011\rangle + |1100\rangle + |1111\rangle \Big)_{3478} \\ &\quad + \Big(|0011\rangle + |1100\rangle \Big)_{1256} \otimes \Big(|0110\rangle + |0101\rangle + |1010\rangle + |1001\rangle \Big)_{3478} \\ &\quad + \Big(|0101\rangle + |1010\rangle \Big)_{1256} \otimes \Big(|0110\rangle - |0101\rangle - |1010\rangle + |1001\rangle \Big)_{3478} \\ &\quad + \Big(|0110\rangle + |1001\rangle \Big)_{1256} \otimes \Big(|0000\rangle - |0011\rangle - |1100\rangle + |1111\rangle \Big)_{3478} \Big]. \end{split}$$
 (E25)

minimizes S_1, S_2, S_3, S_5 and S_7 and maximizes S_6 . Its sector lengths are given by

$$\mathbf{S} = (0, 0, 0, 42, 0, 168, 0, 45). \tag{E26}$$

Its extremality for S_6 has not been established analytically but is supported by our numerics.

Appendix F: Proofs for the dual problem

1. Proof of feasibility Eq. (77)

Here we show that the values given in (78) provide a feasible point of the dual problem, namely that the inequalities $Q_m \geqslant c_m$ hold.

Let us first consider the special case m=N. Equation (76) gives $a_{qN}=0$ for all $q, a'_{kN}=0$ for $k\geqslant 1$ and $a'_{0N}=1/2^N$. We get

$$\sum_{q=1}^{N/2-1} a_{qN} y_q + \sum_{k=0}^{N/2-1} a'_{kN} y'_k = 1 = c_N,$$
 (F1)

thus Eq. (77) holds. For m = 1, ..., N - 1, we only need to show that $Q_m \ge 0$. We have

$$Q_{m} = \delta_{m \text{ even}} \sum_{q=1}^{N/2-1} {N-m \choose 2q+1-m} y_{q} + \sum_{k=0}^{N/2-1} \left[\frac{1}{2^{N-k}} {N-m \choose k} - \frac{1}{2^{k}} {N-m \choose N-k} \right] y'_{k}$$

$$= \delta_{m \text{ even}} \left[2^{1-\frac{N}{2}} {N-m \choose \frac{N}{2}-m} \delta_{N \text{ mod } 4=2} + \sum_{q=\lfloor \frac{N+2}{4} \rfloor}^{\frac{N}{2}-1} {N-m \choose 2q+1-m} 2^{-2q+1} \right] + 1$$

$$+ \sum_{k=1}^{\min(N-m,\frac{N}{2}-1)} \frac{1}{2^{N-k}} {N-m \choose k} \left[(-1)^{k} \left(2^{N-k} - 2^{k} + 1 \right) - 1 \right] - \sum_{k=m}^{N/2-1} \frac{1}{2^{k}} {N-m \choose N-k} \left[(-1)^{k} \left(2^{N-k} - 2^{k} + 1 \right) - 1 \right].$$
(F2)

By replacing m by r = N - m and setting p = N - 2q - 1 in the first sum in (F2), we get for r = 1, ..., N - 1

$$Q_{N-r} = \delta_{r \text{ even}} \left[2^{1-\frac{N}{2}} {r \choose \frac{N}{2}} \delta_{N \text{ mod } 4=2} + \sum_{\substack{p=1 \ p \text{ odd}}}^{2\lfloor \frac{N}{4} \rfloor - 1} 2^{p-N+2} {r \choose p} \right] + 1$$

$$+ \sum_{k=1}^{\min(r, \frac{N}{2} - 1)} \frac{1}{2^{N-k}} {r \choose k} \left[(-1)^k \left(2^{N-k} - 2^k + 1 \right) - 1 \right] - \sum_{k=N-r}^{N/2-1} \frac{1}{2^k} {r \choose N-k} \left[(-1)^k \left(2^{N-k} - 2^k + 1 \right) - 1 \right].$$
(F3)

The sums can be calculated analytically. If $r \leq N/2 - 1$, the last sum is 0 and Eq. (F3) reduces to

$$Q_{N-r} = \delta_r \text{ even } \left[\sum_{\substack{p=1\\ p \text{ odd}}}^{r-1} 2^{p-N+2} \binom{r}{p} \right] + 1 + \sum_{k=1}^r \frac{1}{2^{N-k}} \binom{r}{k} \left[(-1)^k \left(2^{N-k} - 2^k + 1 \right) - 1 \right].$$
 (F4)

The last sum gives

$$\sum_{k=1}^{r} \frac{1}{2^{N-k}} {r \choose k} \left[(-1)^k \left(2^{N-k} - 2^k + 1 \right) - 1 \right] = -1 + \frac{1 - (-3)^r + (-1)^r - 3^r}{2^N}, \tag{F5}$$

while

$$\sum_{\substack{p=1\\ p \text{ odd}}}^{r} 2^p \binom{r}{p} = \frac{1}{2} \left(3^r - (-1)^r \right), \tag{F6}$$

hence (F4) becomes

$$Q_{N-r} = \delta_{r \text{ even}} \left[\frac{3^r - (-1)^r}{2^{N-1}} \right] + \frac{1 - (-3)^r + (-1)^r - 3^r}{2^N} = 0$$
 (F7)

when considering in turn the cases r even and odd.

If $r \ge N/2$, the bounds of the sums are slightly different, and Eq. (F4) becomes

$$Q_{N-r} = \delta_{r \text{ even}} \left[2^{1-\frac{N}{2}} {r \choose \frac{N}{2}} \delta_{N \text{ mod } 4=2} + \sum_{\substack{p=1\\p \text{ odd}}}^{2\lfloor \frac{N}{4} \rfloor - 1} 2^{p-N+2} {r \choose p} \right] + 1$$

$$+ \sum_{k=1}^{\frac{N}{2}-1} \frac{1}{2^{N-k}} {r \choose k} \left[(-1)^k \left(2^{N-k} - 2^k + 1 \right) - 1 \right] - \sum_{k=\frac{N}{2}+1}^{r} \frac{1}{2^{N-k}} {r \choose k} \left[(-1)^k \left(2^k - 2^{N-k} + 1 \right) - 1 \right]$$
(F8)

where in the last sum we changed k to N-k. In the last line, the terms in $(2^{N-k}-2^k)$ give

$$\sum_{k=1}^{r} \frac{1}{2^{N-k}} \binom{r}{k} (-1)^k \left(2^{N-k} - 2^k \right) = -1 + \frac{1 - (-3)^r}{2^N}, \tag{F9}$$

while

$$\sum_{k=1}^{\frac{N}{2}-1} \frac{1}{2^{N-k}} \binom{r}{k} \left[(-1)^k - 1 \right] = -\frac{1}{2^{N-1}} \sum_{k=1 \text{ odd}}^{\frac{N}{2}-1} 2^k \binom{r}{k}$$
 (F10)

$$\sum_{k=\frac{N}{2}+1}^{r} \frac{1}{2^{N-k}} \binom{r}{k} \left[(-1)^k - 1 \right] = -\frac{1}{2^{N-1}} \sum_{\substack{k=\frac{N}{2}+1\\k \text{ odd}}}^{r} 2^k \binom{r}{k}.$$
 (F11)

The difference of the above two identities yields

$$\sum_{k=1}^{\frac{N}{2}-1} \frac{1}{2^{N-k}} \binom{r}{k} \left[(-1)^k - 1 \right] - \sum_{k=\frac{N}{2}+1}^r \frac{1}{2^{N-k}} \binom{r}{k} \left[(-1)^k - 1 \right]$$
 (F12)

$$= -\frac{1}{2^{N-1}} \sum_{\substack{k=1\\k \text{ odd}}}^{\frac{N}{2}-1} 2^k \binom{r}{k} + \frac{1}{2^{N-1}} \sum_{\substack{k=\frac{N}{2}+1\\k \text{ odd}}}^{r} 2^k \binom{r}{k}$$
 (F13)

$$= \frac{1}{2^{N-1}} \left(-2 \sum_{\substack{k=1\\k \text{ odd}}}^{\frac{N}{2}-1} 2^k \binom{r}{k} - 2^{\frac{N}{2}} \binom{r}{\frac{N}{2}} \delta_{N \text{ mod } 4=2} + \sum_{\substack{k=1\\k \text{ odd}}}^{r} 2^k \binom{r}{k} \right).$$
 (F14)

(F14)

We thus get

$$Q_{N-r} = \delta_{r \text{ even}} \left[2^{1-\frac{N}{2}} {r \choose \frac{N}{2}} \delta_{N \text{ mod } 4=2} + \sum_{\substack{k=1\\k \text{ odd}}}^{2\left\lfloor \frac{N}{4} \right\rfloor - 1} 2^{k-N+2} {r \choose k} \right] + \frac{1 - (-3)^r}{2^N}$$

$$- 2^{2-N} \sum_{\substack{k=1\\k \text{ odd}}}^{\frac{N}{2} - 1} 2^k {r \choose k} - 2^{1-\frac{N}{2}} {r \choose \frac{N}{2}} \delta_{N \text{ mod } 4=2} + \frac{3^r - (-1)^r}{2^N}$$
 (F15)

(using (F6) for the last term). For even r and $N=4M+2\epsilon$, $\epsilon=0,1$, the upper bounds of the remaining sums are respectively 2M-1 and $2M-1+\epsilon$, but since the sums run over odd k only, the two sums cancel whether $\epsilon=0$ or 1; thus $Q_{N-r}=0$ for even r. For odd r, Eq. (F15) reduces to

$$Q_{N-r} = \frac{1}{2^{N-2}} \left(\frac{1+3^r}{2} - \sum_{\substack{k=1\\k \text{ odd}}}^{\frac{N}{2}-1} 2^k \binom{r}{k} - 2^{\frac{N}{2}-1} \binom{r}{\frac{N}{2}} \delta_{N \text{ mod } 4=2} \right)$$

$$= \frac{1}{2^{N-2}} \left(\sum_{\substack{k=\frac{N}{2}\\k \text{ odd}}}^{r} 2^k \binom{r}{k} - \frac{1}{2} 2^{\frac{N}{2}} \binom{r}{\frac{N}{2}} \delta_{N \text{ mod } 4=2} \right),$$
(F16)

where we used again Eq. (F6). It is a sum of positive terms, apart from the last term, which, for N/2 odd, is half the term corresponding to k = N/2 in the sum. Therefore $Q_{N-r} \ge 0$.

2. Proof of Eq. (80)

We have

$$b_q = (2^{2q} - 1) \binom{N}{2q+1}, \qquad b'_k = \frac{2^{N-k} - 2^k}{2^N} \binom{N}{k}.$$
 (F17)

Using the values (78) for y_q, y'_k , we get

$$\sum_{q=1}^{N/2-1} b_q y_q + \sum_{k=0}^{N/2-1} b_k' y_k' = \left(1 - 2^{1 - \frac{N}{2}}\right) {N \choose \frac{N}{2}} \delta_{N \bmod 4 = 2} + 2 \sum_{q=\lfloor \frac{N+2}{4} \rfloor}^{\frac{N}{2} - 1} (1 - 2^{-2q}) {N \choose 2q + 1} + 2^N - 1 + \frac{1}{2^N} \sum_{k=1}^{\frac{N}{2} - 1} (2^{N-k} - 2^k) {N \choose k} \left[(-1)^k (2^{N-k} - 2^k + 1) - 1 \right].$$
(F18)

The first sum is

$$2\sum_{q=\lfloor \frac{N+2}{4} \rfloor}^{\frac{N}{2}-1} (1-2^{-2q}) {N \choose 2q+1} = 2\sum_{\substack{k=1\\k \text{ odd}}}^{\frac{N}{2}-1} (1-2^{-N+k+1}) {N \choose k},$$
 (F19)

while the second sum reads

$$\sum_{\substack{k=1\\k \text{ odd}}}^{\frac{N}{2}-1} {N \choose k} \left(2^{-k} - 2^{k-N}\right) \left(2^k - 2^{N-k} - 2\right) + \frac{1}{2^N} \sum_{\substack{k=2\\k \text{ odd}}}^{\frac{N}{2}-1} {N \choose k} \left(2^{N-k} - 2^k\right)^2.$$
 (F20)

Summing up Eqs. (F19) and (F20) gives

$$\sum_{\substack{k=1\\k \text{ odd}}}^{\frac{N}{2}-1} {N \choose k} \left(4 - 2^{-N+k+1} - 2^{2k-N} - 2^{N-2k} - 2^{1-k}\right) + \frac{1}{2^N} \sum_{\substack{k=2\\k \text{ even}}}^{\frac{N}{2}-1} {N \choose k} \left(2^{N-k} - 2^k\right)^2.$$
 (F21)

For the second sum we get

$$\sum_{k=2 \atop k \text{ even}}^{\frac{N}{2}-1} {N \choose k} (2^{N-k} - 2^k)^2 = \sum_{k=2 \atop k \text{ even}}^{N} {N \choose k} (2^{N-k} - 2^k)^2 - \sum_{k=\frac{N}{2} \atop k \text{ even}}^{N} {N \choose k} (2^{N-k} - 2^k)^2$$
 (F22)

$$= \sum_{\substack{k=2\\k \text{ even}}}^{N} {N \choose k} (2^{N-k} - 2^k)^2 - \sum_{\substack{k=0\\k \text{ even}}}^{\frac{N}{2}} {N \choose k} (2^k - 2^{N-k})^2$$
 (F23)

and thus

$$\sum_{k=2 \atop k \text{ even}}^{\frac{N}{2}-1} {N \choose k} \left(2^{N-k}-2^k\right)^2 = \frac{1}{2} \sum_{k=2 \atop k \text{ even}}^{N} {N \choose k} \left(2^{N-k}-2^k\right)^2 - \left(1-2^N\right)^2 = \frac{5^N+3^N-3\times 4^N+2^{N+2}-2}{2}.$$
 (F24)

For the odd terms in (F21), and in the same way changing k to N-k, we obtain

$$\sum_{\substack{k=1\\k \text{ odd}}}^{\frac{N}{2}-1} {N \choose k} \left(4 - 2^{-N+k+1} - 2^{2k-N} - 2^{N-2k} - 2^{1-k}\right) = \sum_{\substack{k=\frac{N}{2}+1\\k \text{ odd}}}^{N-1} {N \choose k} \left(4 - 2^{-k+1} - 2^{N-2k} - 2^{2k-N} - 2^{1-N+k}\right). \tag{F25}$$

Thus, adding both sides and dividing by 2,

$$\sum_{k=1 \atop k \text{ odd}}^{\frac{N}{2}-1} {N \choose k} \left(4 - 2^{-N+k+1} - 2^{2k-N} - 2^{N-2k} - 2^{1-k}\right) \\
= \frac{1}{2} \sum_{k=1 \atop k \text{ odd}}^{N-1} {N \choose k} \left(4 - 2^{-k+1} - 2^{N-2k} - 2^{2k-N} - 2^{1-N+k}\right) - {N \choose \frac{N}{2}} (1 - 2^{-\frac{N}{2}+1}) \delta_{N \text{ mod } 4=2} \\
= \frac{2^{2N+1} - 3^N - 5^N + 2}{2^{N+1}} - {N \choose \frac{N}{2}} (1 - 2^{-\frac{N}{2}+1}) \delta_{N \text{ mod } 4=2}.$$

Gathering together all identities, Eq. (80) yields

$$\sum_{q=1}^{N/2-1} b_q y_q + \sum_{k=0}^{N/2-1} b_k' y_k' = 2^N - 1 + \frac{5^N + 3^N - 3 \times 4^N + 2^{N+2} - 2}{2^{N+1}} + \frac{2^{2N+1} - 3^N - 5^N + 2}{2^{N+1}}$$

$$= 2^{N-1} + 1,$$
(F26)

which completes the proof.

[1] D. Bruß, Phys. Rev. A 60, 4344 (1999).

- [7] W. Laskowski, D. Richart, C. Schwemmer, T. Paterek, and H. Weinfurter, Phys. Rev. Lett. 108, 240501 (2012).
- [8] C. Eltschka, F. Huber, O. Gühne, and J. Siewert, Phys. Rev. A 98, 052317 (2018).
- [9] F. Mintert, M. Kuś, and A. Buchleitner, Phys. Rev. Lett. 95, 260502 (2005).
- [10] M. Markiewicz, W. Laskowski, T. Paterek, and M. Żukowski, Phys. Rev. A 87, 034301 (2013).
- [11] C. Eltschka and J. Siewert, Phys. Rev. Lett. 114, 140402 (2015).

^[2] V. Coffman, J. Kundu, and W. K. Wootters, Phys. Rev. A 61, 052306 (2000).

^[3] H. Aschauer, J. Calsamiglia, M. Hein, and H.-J. Briegel, Quantum Information and Computation 4, 383 (2004).

^[4] M. C. Tran, B. Dakić, W. Laskowski, and T. Paterek, Phys. Rev. A 94, 042302 (2016).

^[5] N. Wyderka and O. Gühne, Journal of Physics A: Mathematical and Theoretical **53**, 345302 (2020).

^[6] R. Horodecki, P. Horodecki, and M. Horodecki, Physics Letters A 210, 377 (1996).

- [12] J. Tura, A. Aloy, F. Baccari, A. Acín, M. Lewenstein, and R. Augusiak, Phys. Rev. A 100, 032307 (2019).
- [13] M. Miller and D. Miller, in 2021 IEEE International Conference on Quantum Computing and Engineering (QCE) (2021) pp. 378–384.
- [14] S. Wehner and A. Winter, Journal of Mathematical Physics 49, 062105 (2008).
- [15] C. de Gois, K. Hansenne, and O. Gühne, Phys. Rev. A 107, 062211 (2023).
- [16] M. B. Morán and F. Huber, Phys. Rev. Lett. 132, 200202 (2024).
- [17] W. Helwig, W. Cui, J. I. Latorre, A. Riera, and H.-K. Lo, Phys. Rev. A 86, 052335 (2012).
- [18] F. Huber and S. Severini, Journal of Physics A: Mathematical and Theoretical 51, 435301 (2018).
- [19] D. Miller, D. Loss, I. Tavernelli, H. Kampermann, D. Bruß, and N. Wyderka, Journal of Physics A: Mathematical and Theoretical 56, 335303 (2023).
- [20] P. Cieśliński, S. Imai, J. Dziewior, O. Gühne, L. Knips, W. Laskowski, J. Meinecke, T. Paterek, and T. Vértesi, Physics Reports 1095, 1 (2024).
- [21] P. Shor and R. Laflamme, Phys. Rev. Lett. 78, 1600 (1997).
- [22] A. J. Scott, Phys. Rev. A 69, 052330 (2004).
- [23] A. Ekert and C. Macchiavello, Phys. Rev. Lett. 77, 2585 (1996).
- [24] N. J. Cerf and R. Cleve, Phys. Rev. A 56, 1721 (1997).
- [25] E. Rains, IEEE Transactions on Information Theory 44, 1388 (1998).
- [26] A. Calderbank, E. Rains, P. Shor, and N. Sloane, IEEE Transactions on Information Theory 44, 1369 (1998).
- [27] E. Rains, IEEE Transactions on Information Theory 45, 2361 (1999).
- [28] E. Rains, IEEE Transactions on Information Theory 46, 54 (2000).
- [29] D. Miller, K. Levi, L. Postler, A. Steiner, L. Bittel, G. A. L. White, Y. Tang, E. J. Kuehnke, A. A. Mele, S. Khatri, L. Leone, J. Carrasco, C. D. Marciniak, I. Pogorelov, M. Guevara-Bertsch, R. Freund, R. Blatt, P. Schindler, T. Monz, M. Ringbauer, and J. Eisert, Experimental measurement and a physical interpretation of quantum shadow enumerators (2024), arXiv:2408.16914 [quant-ph].
- [30] N. Gisin and H. Bechmann-Pasquinucci, Physics Letters A 246, 1 (1998).
- [31] A. Higuchi and A. Sudbery, Physics Letters A 273, 213 (2000).
- [32] İ. D. K. Brown, S. Stepney, A. Sudbery, and S. L. Braunstein, Journal of Physics A: Mathematical and General 38, 1119 (2005).
- [33] A. Borras, A. R. Plastino, J. Batle, C. Zander, M. Casas, and A. Plastino, Journal of Physics A: Mathematical and Theoretical 40, 13407 (2007).
- [34] F. Huber, O. Gühne, and J. Siewert, Phys. Rev. Lett. 118, 200502 (2017).
- [35] F. Huber, C. Eltschka, J. Siewert, and O. Gühne, Journal of Physics A: Mathematical and Theoretical 51, 175301 (2018).
- [36] M. Grassl, T. Beth, and M. Rötteler, International Journal of Quantum Information 02, 55 (2004).
- [37] L. Arnaud and N. J. Cerf, Phys. Rev. A 87, 012319 (2013).
- [38] D. Goyeneche and K. Życzkowski, Phys. Rev. A 90, 022316 (2014).

- [39] W. Kłobus, A. Burchardt, A. Kołodziejski, M. Pandit, T. Vértesi, K. Życzkowski, and W. Laskowski, Phys. Rev. A 100, 032112 (2019).
- [40] X. Zhang, S. Pang, S.-M. Fei, and Z.-J. Zheng, Advanced Quantum Technologies 7, 2400245 (2024).
- [41] W. Zhang, Y. Ning, F. Shi, and X. Zhang, Extremal maximal entanglement (2024), arXiv:2411.12208 [quant-ph].
- [42] Y. Ning, F. Shi, T. Luo, and X. Zhang, Linear programming bounds on k-uniform states (2025), arXiv:2503.02222 [quant-ph].
- [43] M. Enríquez, I. Wintrowicz, and K. Życzkowski, Journal of Physics: Conference Series 698, 012003 (2016).
- [44] E. Knill and R. Laflamme, Phys. Rev. A 55, 900 (1997).
- [45] S. Bravyi, Phys. Rev. A 67, 012313 (2003).
- [46] F. Huber and M. Grassl, Quantum 4, 284 (2020).
- [47] O. Giraud, D. Braun, D. Baguette, T. Bastin, and J. Martin, Phys. Rev. Lett. 114, 080401 (2015).
- [48] A. Wong and N. Christensen, Phys. Rev. A 63, 044301 (2001).
- [49] M. Krawtchouk, Compt. Rend. 189, 620 (1929).
- [50] V. Levenshtein, IEEE Transactions on Information Theory 41, 1303 (1995).
- [51] C. Eltschka and J. Siewert, Quantum 4, 229 (2020).
- [52] G. Gour and N. R. Wallach, Journal of Mathematical Physics 51, 112201 (2010).
- [53] G. Gour, S. Bandyopadhyay, and B. C. Sanders, Journal of Mathematical Physics 48, 012108 (2007).
- [54] S. P. Boyd and L. Vandenberghe, Convex optimization (Cambridge university press, 2004).
- [55] F. J. MacWilliams and N. J. A. Sloane, The theory of error-correcting codes (North-Holland Publishing Company, New York, 1977).
- [56] J. Conway and N. Sloane, IEEE Transactions on Information Theory 36, 1319 (1990).
- [57] F. Mintert and A. Buchleitner, Phys. Rev. Lett. 98, 140505 (2007).
- [58] R. Demkowicz-Dobrzański, A. Buchleitner, M. Kuś, and F. Mintert, Phys. Rev. A 74, 052303 (2006).
- [59] I. G. Macdonald, Symmetric functions and Hall polynomials (Oxford university press, 1998).
- [60] S. S. Bullock and G. K. Brennen, Journal of Mathematical Physics 45, 2447 (2004).
- [61] C. Eltschka, T. Bastin, A. Osterloh, and J. Siewert, Phys. Rev. A 85, 022301 (2012).
- [62] E. Majorana, Nuovo Cimento 9, 43 (1932).
- [63] J. Zimba, Electronic Journal of Theoretical Physics 3, 143 (2006).
- [64] M. Aulbach, D. Markham, and M. Murao, New Journal of Physics 12, 073025 (2010).
- [65] J. Martin, O. Giraud, P. A. Braun, D. Braun, and T. Bastin, Phys. Rev. A 81, 062347 (2010).
- [66] D. Baguette, T. Bastin, and J. Martin, Phys. Rev. A 90, 032314 (2014).
- [67] F. Huber, Table of AME states, https://huberfe.github.io/ame (2024).
- [68] X.-w. Zha, H.-y. Song, J.-x. Qi, D. Wang, and Q. Lan, Journal of Physics A: Mathematical and Theoretical 45, 255302 (2012).
- [69] X. Zha, C. Yuan, and Y. Zhang, Laser Physics Letters 10, 045201 (2013).
- [70] X. Zha, Z. Da, I. Ahmed, and Y. Zhang, Laser Physics Letters 15, 055206 (2018).

$\begin{array}{ c c c } \hline N\geqslant 2 & \hline \\ \hline & 2 & \hline \\ \hline \end{array}$	0ª	-	1								
	0ª	LOTTE (AT))	m=1					N=2			
2		$ \mathrm{GHZ}(N)\rangle$	$N^{\mathbf{b}}$	$ 0\rangle^{\otimes N}$	1	0ª	$ \mathrm{GHZ}(2)\rangle$	2 ^b	$ 0\rangle^{\otimes 2}$		
2	m=2			2	1°	$ 0\rangle^{\otimes 2}$	3 ^b	$ \mathrm{GHZ}(2)\rangle$			
				N=3							
3	3^{b}	any $ \psi\rangle$	3 ^b	any $ \psi\rangle$	1	0ª	$ \mathrm{GHZ}(3)\rangle$	3 ^b	$ 0\rangle^{\otimes 3}$		
4	$2^{\mathbf{d}}$	$ { m tetra} angle$	6 ^b	$ 0\rangle^{\otimes 4}$	2	3 ^b	any $ \psi\rangle$	3 ^b	any $ \psi\rangle$		
5	$0^{\mathbf{e}}$	$ AME(5,2)\rangle^{(E4)}$	10 ^b	$ 0\rangle^{\otimes 5}$	3	1°	$ 0\rangle^{\otimes 3}$	4 ^c	$ \mathrm{GHZ}(3)\rangle$		
6	$0^{\mathbf{e}}$	$ AME(6,2)\rangle^{(E8)}$	15 ^b	$ 0\rangle^{\otimes 6}$		•	N =	4			
7	0	$ AME(6,2)\rangle 0\rangle$	21 ^b	$ 0\rangle^{\otimes 6}$	1	0ª	$ \mathrm{GHZ}(4)\rangle$	4 ^b	$ 0\rangle^{\otimes 4}$		
8	0	$ \psi_{M}\rangle_{12783456}^{(E20)}$	28 ^b	$ 0\rangle^{\otimes 8}$	2	2 ^d	$ { m tetra} angle$	6 ^b	$ 0 angle^{\otimes 4}$		
$N \geqslant 9$?	?	$\binom{N}{2}^{\mathbf{b}}$	$ 0\rangle^{\otimes N}$	3	$0^{\mathbf{a}}$	$ \mathrm{GHZ}(4)\rangle$	8 ^b	$ { m tetra} angle$		
		m = 3	3		4	1°	$ 0\rangle^{\otimes 4}$	9 _p	$ \mathrm{GHZ}(4)\rangle$		
3	1°	$ 0\rangle^{\otimes 3}$	4 ^c	$ \mathrm{GHZ}(3)\rangle$			N =	5			
4	$0^{\mathbf{a}}$	$ \mathrm{GHZ}(4)\rangle$	8 ^b	$ ext{tetra}\rangle$	1	0ª	$ GHZ(5)\rangle$	5 ^b	$ 0\rangle^{\otimes 5}$		
$N \geqslant 5$	$0^{\mathbf{a}}$	$ \mathrm{GHZ}(N)\rangle$	$\binom{N}{3}^{\mathbf{b}}$	$ 0\rangle^{\otimes N}$	2	0 ^e	$ AME(5,2)\rangle$	10 ^b	$ 0\rangle^{\otimes 5}$		
				1 /	3	$0^{\mathbf{a}}$	$ \mathrm{GHZ}(5)\rangle$	10 ^b	$ 0\rangle^{\otimes 5}$		
4	1.0	m = 4		lour(4))	4	5	$ 0\rangle^{\otimes 5}$	15	$ \mathrm{AME}(5,2)\rangle$		
4	1°	$ 0\rangle^{\otimes 4}$	9 ^b	$ GHZ(4)\rangle$	5	1°	$ 0\rangle^{\otimes 5}$	16 ^c	$ \mathrm{GHZ}(5)\rangle$		
	5 $ 0\rangle^{\otimes 5}$ 15 $ AME(5,2)\rangle$				N=6						
$\begin{bmatrix} 6 \\ 7 \end{bmatrix}$	5 7	$ \mathrm{GHZ}(5)\rangle 0\rangle$ $ \psi_7\rangle^{(\mathrm{E}14)}$	45 45	$ AME(6,2)\rangle$ $ AME(6,2)\rangle 0\rangle$	1	0ª	$ \mathrm{GHZ}(6)\rangle$	6 ^b	$ 0\rangle^{\otimes 6}$		
8	14	$ \psi_7\rangle^{(1)}$ $ ext{tetra}\rangle^{\otimes 2}$	70	$ AME(0,2)/ 0\rangle$ $ 0\rangle^{\otimes 8}$	2	0 ^e	$ \mathrm{AME}(6,2)\rangle$	15 ^b	$ 0\rangle^{\otimes 6}$		
0	14			0) -	3	$0^{\mathbf{a}}$	$ \mathrm{GHZ}(6)\rangle$	20 ^b	$ 0\rangle^{\otimes 6}$		
	4.C	m = 3		lorra(z))	4	5	$ \mathrm{GHZ}(5)\rangle 0\rangle$	45	$ AME(6,2)\rangle$		
5	1°	$ 0\rangle^{\otimes 5}$	16°	$ GHZ(5)\rangle$	5	$0^{\mathbf{a}}$	$ \mathrm{GHZ}(6)\rangle$	24	$ pyramid\rangle^{(E12)}$		
6	$0^{\mathbf{a}}$ $0^{\mathbf{a}}$	$ GHZ(6)\rangle$	24	$ \text{pyramid}\rangle^{\text{(E12)}}$ $ \psi_{7b}\rangle^{\text{(E18)}}$	6	1^{c}	$ 0\rangle^{\otimes 6}$	33 ^b	$ \mathrm{GHZ}(6)\rangle$		
$\begin{bmatrix} 7 \\ 8 \end{bmatrix}$	0 0ª	$ \mathrm{GHZ}(7)\rangle$ $ \mathrm{GHZ}(8)\rangle$	603/13 90	$ \Psi^{7b}\rangle$ $ AME(6,2)\rangle 0\rangle^{\otimes 2}$	N=7						
	$0^{\mathbf{a}}$	$ \operatorname{GHZ}(\delta)\rangle$	90 ?	?	1	0ª	$ \mathrm{GHZ}(7)\rangle$	7 ^b	$ 0\rangle^{\otimes 7}$		
7 1 ()//		2	0	$ AME(6,2)\rangle 0\rangle$	21 ^b	$ 0\rangle^{\otimes 7}$					
0	1.0	m = 0		CII7(6)	3	$0^{\mathbf{a}}$	$ \mathrm{GHZ}(7)\rangle$	35 ^b	$ 0\rangle^{\otimes 7}$		
6	1°	$ 0\rangle^{\otimes 6}$	33 ^b	$ GHZ(6)\rangle$	4	7	$ \psi_7\rangle^{(\text{E}14)}$	45	$ AME(6,2)\rangle 0\rangle$		
7	7	$ 0\rangle^{\otimes 7}$	49	$ \psi_7\rangle^{(\text{E}14)}$	5	$0^{\mathbf{a}}$	$ \mathrm{GHZ}(7)\rangle$	603/13	$ \psi_{7b}\rangle^{(\text{E}18)}$		
8	7	$ \mathrm{GHZ}(7)\rangle 0\rangle$	168	$ \psi^{1}_{12345678}\rangle^{(E25)}$	6	7	$ 0\rangle^{\otimes 7}$	49	$ \psi_7 angle^{({ m E}14)}$		
m = 7				7	1 ^c	$ 0\rangle^{\otimes 7}$	64 ^c	$ \mathrm{GHZ}(7)\rangle$			
7	1°	$ 0\rangle^{\otimes 7}$	64°	$ GHZ(7)\rangle$			N =	8			
8	0ª	$ GHZ(8)\rangle$	592/7	$ \text{tetra}(8)\rangle^{(\text{E22})}$	1	0ª	GHZ(8)	8 ^b	$ 0\rangle^{\otimes 8}$		
$N \geqslant 9$	0ª	$ \mathrm{GHZ}(8)\rangle$?	?	2	0	$ \psi_M\rangle_{12783456}^{(E20)}$	28 ^b	$ 0\rangle^{\otimes 8}$		
		m = 3			3	$0^{\mathbf{a}}$	$ \mathrm{GHZ}(8)\rangle$	56 ^b	$ 0\rangle^{\otimes 8}$		
8	1 ^c	$ 0\rangle^{\otimes 8}$	129 ^b	$ \mathrm{GHZ}(8)\rangle$	4	14	$ \text{tetra}\rangle^{\otimes 2}$	70	$ 0\rangle^{\otimes 8}$		
m = N				5	$0^{\mathbf{a}}$	$ \mathrm{GHZ}(8)\rangle$	90	$ AME(6,2)\rangle 0\rangle^{\otimes 2}$			
N odd	1 ^c	$ 0\rangle^{\otimes N}$	2^{N-1c}	$ \mathrm{GHZ}(N)\rangle$	6	7	$ \mathrm{GHZ}(7)\rangle 0\rangle$	168	$ \psi^{1}_{12345678}\rangle^{(E25)}$		
N even	1^{c}	$ 0\rangle^{\otimes N}$	$2^{N-1} + 1^{\mathbf{f}}$	$ \mathrm{GHZ}(N)\rangle$	7	0ª	$ \mathrm{GHZ}(8)\rangle$	592/7	$ \text{tetra}(8)\rangle^{(E22)}$		
$a S_m \ge 0$ $b [5]$ $c [4]$ $d [22, 31]$ $e [17, 33, 67]$ $f [51]$ 8					8	1°	$ 0\rangle^{\otimes 8}$	129 ^b	$ \mathrm{GHZ}(8)\rangle$		

TABLE III. Examples of optimal N-qubit pure states that extremize the sector lengths S_m (4), presented in two tables: one sorted by N (left) and the other by m (right). The footnotes refer to trivial inequalities or previous work identifying some of these optimal states and rigorously proving their optimality. All states whose optimality is proven appear in a grey cell. They correspond to the extreme values of the region \mathcal{R} [see Eq. (38)], and therefore of the pure-states numerical range \mathcal{S} [see Eq. (21)]. All other states are putative optima, identified using algebraic-numerical methods and sometimes corresponding to states known in the literature, but they lack a formal proof of optimality.

N	$(N_A,N_{ar{A}})$	$\min[\operatorname{Tr}(\rho_A^2) + R_{\rho_A}]$	optimal state	$(\operatorname{Tr}(\rho_A^2), R_{\rho_A})$
2	(1,1)	1	any $ \psi\rangle$	$(x, 1-x)^{a}$
3	(2,1)	2^{-1}	$ 0\rangle \mathrm{GHZ}(2)\rangle$	$(2^{-1},0)$
4	(3,1)	2^{-1}	$ 0\rangle GHZ(3)\rangle$	$(2^{-1},0)$
5	(4,1)	2^{-1}	$ 0\rangle \mathrm{GHZ}(4)\rangle$	$(2^{-1},0)$
6	(5,1)	2^{-1}	$ 0\rangle \mathrm{GHZ}(5)\rangle$	$(2^{-1},0)$
3	(1,2)	1	any $ \psi\rangle$	(x, 1 - x)
4	(2,2)	2^{-1}	$ 0\rangle \mathrm{GHZ}(3)\rangle$	$(2^{-1},0)$
5	(3,2)	2^{-2}	$ AME(5,2)\rangle$	$(2^{-2},0)$
6	(4,2)	2^{-2}	$ 0\rangle \mathrm{AME}(5,2)\rangle$	$(2^{-2},0)$
7	(5,2)	2^{-2}	$ \mathrm{GHZ}(2)\rangle \mathrm{AME}(5,2)\rangle$	$(2^{-2},0)$
8	(6,2)	2^{-2}	$ 0\rangle^{\otimes 2} \mathrm{AME}(6,2)\rangle$	$(2^{-2},0)$
9	(7,2)	2^{-2}	$ 0\rangle^{\otimes 3} \mathrm{AME}(6,2)\rangle$	$(2^{-2},0)$
4	(1,3)	1	any $ \psi\rangle$	(x, 1 - x)
5	(2,3)	2^{-1}	$ \mathrm{AME}(5,2)\rangle^{(\mathbf{E4})}$	$(2^{-2}, 2^{-2})$
6	(3,3)	2^{-2}	$ \mathrm{AME}(6,2)\rangle^{(\mathrm{E8})}$	$(2^{-3}, 2^{-3})$
7	(4,3)	2^{-3}	$ 0\rangle AME(6,2)\rangle$	$(2^{-3},0)$
8	(5,3)	2^{-3}	$ 0\rangle^{\otimes 2} \mathrm{AME}(6,2)\rangle$	$(2^{-3},0)$
9	(6,3)	2^{-3}	$ 0\rangle^{\otimes 3} \mathrm{AME}(6,2)\rangle$	$(2^{-3},0)$
5	(1,4)	1	any $ \psi\rangle$	(x, 1 - x)
6	(2,4)	2^{-1}	$ \mathrm{AME}(6,2)\rangle$	$(2^{-2}, 2^{-2})$
7	(3,4)	2^{-2}	$ 0\rangle \mathrm{AME}(6,2)\rangle$	$(2^{-2},0)$
8	(4,4)	2^{-3}	$ 0\rangle \psi_{M}\rangle_{1234567}^{(E16)}$	$(2^{-3},0)$
9	(5,4)	2^{-4}	numerical	$(2^{-4},0)$
10	(6,4)	2^{-4}	numerical	$(2^{-4},0)$
6	(1,5)	1	any $ \psi\rangle$	(x, 1 - x)
7	(2,5)	2^{-1}	$ AME(6,2)\rangle 0\rangle$	$(2^{-2}, 2^{-2})$
8	(3,5)	2^{-2}	$ \mathrm{AME}(6,2)\rangle 0\rangle^{\otimes 2}$	$(2^{-3}, 2^{-3})$
9	(4,5)	2^{-3}	$ 0\rangle \psi_{M}\rangle_{12783456}^{(E20)}$	$(2^{-3},0)$
10	(5,5)	2-4	numerical	(0.04787, 0.01463)

 $^{^{\}mathrm{a}}$ with $x \in [1/2,1]$

TABLE IV. Examples of states that minimize $\text{Tr}(\rho_A^2) + R_{\rho_A}$. For $N_A > N_{\bar{A}}$ (i.e., k > N - k), the minimum coincides with the lower bound $2^{-\min(k,N-k)}$ presented in Eq. (28), which is therefore saturated by the corresponding optimal state. All states whose optimality is rigorously proven appear in a grey cell, the others being putative optimal states obtained by numerical optimization.